One-Electron Theory of Metals. Cohesive and Structural Properties

Skriver, Hans Lomholt

Publication date:
1984

Document Version
Publisher's PDF, also known as Version of record

Citation (APA):
Skriver, H. L. (1984). One-Electron Theory of Metals. Cohesive and Structural Properties. Danmarks Tekniske Universitet, Risø Nationallaboratoriet for Bæredygtig Energi. (Denmark. Forskningscenter Risoe. Risoe-R; No. 516).

Risø-R-516

RISØ

Risø-R-516

One-Electron Theory of Metals
Cohesive and structural properties

Hans L. Skriver

Risø National Laboratory, DK-4000 Roskilde, Denmark
December 1984

D: 8510082774

RISØ-R-516

ONE-ELECTRON THEORY OF METALS

Cohesive and structural properties

Hans L. Skriver

Abstract. The work described in the report and the 16 accompanying publications is based upon a one-electron theory obtained within the local approximation to density-functional theory, and deals with the ground state of metals as obtained from self-consistent electronic-structure calculations performed by means of the Linear Muffin-Tin Orbital (LMTO) method. It has been the goal of the work to establish how well this one-electron approach describes physical properties such as the crystal structures of the transition metals, the structural phase transitions in the alkali, alkaline earth, and rare earth metals, and the localization of 3d, 4f, and 5f electrons in the 3d metal monoxides, the light lanthanides, and the actinides, respectively, as well as the cohesive properties of metals in general.

December 1984
Risø National Laboratory, DK-4000 Roskilde, Denmark

ISBN 87-550-1136-5
ISSN 0106-2840

Grafisk Service Center, Risø 1985

CONTENT Page

PREFACE

The present thesis together with the 16 previously published papers listed below has been submitted to the Natural Science Faculty of the University of Copenhagen for defence in fulfilment of the requirements for the degree of Dr. of Science. It is closely related to the review of one-electron calculations of the crystal structures of metals which will appear in the Festskrift published by the Royal Danish Academy of Sciences and Letters to commemorate the centennial of Niels Bohr's birth.

The work described in the thesis and the 16 accompanying publications is based upon a one-electron theory obtained within the local approximation to density-functional theory, and deals with the ground state of metals as obtained from self-consistent electronic-structure calculations performed by means of the Linear Muffin-Tin Orbital (LMTO) method. It has been the goal of the work to establish how well such a one-electron approach can describe so different physical properties as the crystal structures of the transition metals, the structural phase transitions in the alkali, alkaline earth, and rare earth metals, and the localization of 3d, 4f, and 5f electrons in the 3d metal monoxides, the light lanthanides, and the actinides, respectively, as well as the cohesive properties of metals in general.

It would not have been possible to complete such a relatively extensive study of the metallic elements, which has included several thousand energy-band calculations, without the advent of the linear methods of band theory due to O. K. Andersen. In the present work I have used these methods as expedient means to perform the necessary self-consistent electronic structure calculations, allowing me to reach my objectives with relatively modest computational efforts. It should be realized, however, that establishing the range of usefulness of one-electron theory is only one step, although an important one, towards the understanding of metallic behaviour, the next step being a pedagogical one in which one builds simple models to make the complete calculations more intelligible. This latter step has been given little attention in the present study.

The course of the present study has been influenced by advice and comments from many of my collegues. Thus, at a very early stage I obtained from Ole Krogh Andersen a copy of his unpublished notes dealing with the LMTO method which I subsequently turned into computer codes while at The National Research Council of Canada in Ottawa and The Kamerlingh Onnes Laboratory in Leiden. Upon my return to Denmark I joined the small band-structure group at Risø National Laboratory, and in collaboration with O. K. Andersen set out to develop self-consistent energy-band programs for magnetically ordered intermetallic compounds. At this stage Börje Johansson drew our attention to the peculiar behaviour of the atomic volume of the actinide metals, and we realized that with the capability to do spin-polarized calculations we might be able to explain the anomaly found experimentally between plutonium and americum. Later, at The Max Planck Institute in Stuttgart I extended these calculations to include the 3d monoxides and antiferromagnetic chromium.

In the above-mentioned calculations I had been using the so-called pressure formula to estimate atomic volumes and bulk modulii. Prior to that O. K. Andersen had formulated his related force relation, and during the calculations on calcium I realized that the experimentally observed pressure-induced structural-phase transitions in the alkaline earth metals could be explained on the basis of the structural energy-differences obtained by means of this force relation. It was this realization which subsequently led to the investigation of the crystal structures of all metals to the left of the zinc group in the periodic table included in the present thesis.

It is a pleasure to thank my two foremost collaborators Ole Krogh Andersen and Börje Johansson for helping me along the somewhat convoluted path outlined above. I have also benefitted greatly from discussions with Ove Jepsen and Niels Egede Christensen, and especially by access to the LMTO, state density, and other computer programs developed by them and by Uffe K. Poulsen and Jan Madsen. In addition I would like to thank Heinz Nohl, Allan MacDonald, and Andy McMahan all of whom at one time or another have worked with me on particular calculations. In this context I am especially grateful to Jean-Pierre Jan who was a true collaborator until his untimely death in 1981. Finally, I wish to thank my colleagues at Risø National Laboratory as well as those at the many other institutions where I have been working during the last seven years for providing me with excellent working conditions.

The present work would not have existed without the financial support from Risø National Laboratory, The Max Planck Institut für Festkörperforschung, NORDITA, Los Alamos Scientific Laboratory, and The Danish Natural Science Foundation as well as the Niels Bohr Foundation and The Royal Danish Academy of Sciences and Letters. Their support is greatly appreciated.

INCLUDED PUBLICATIONS

I1. Calculated bulk properties of the actinide metals.
H.L. Skriver, O.K. Andersen, and B. Johansson, Phys. Rev. Lett. 41, 42 (1978).

I2. Electronic structure of transition metal compounds; ground state properties of the 3d-monoxides in the atomic sphere approximation.
O.K. Andersen, H.L. Skriver, H. Nohl, and B. Johansson, Pure and Appl. Chem. 52, 93 (1980).

I3. Electronic states in thorium under pressure.
H.L. Skriver and J.-P. Jan, Phys. Rev. B21, 1489 (1980).

I4. Prediction of Fermi surface pressure dependence in Rb and Cs.
J.-P. Jan, A.H. MacDonald, and H.L. Skriver, Phys. Rev. B21, 5584 (1980).

I5. 5-f delocalization in americum.
H.L. Skriver, O.K. Andersen, and B. Johansson, Phys. Rev. Lett. 44, 1230 (1980).

I6. Electronic structure of antiferromagnetic chromium.
H.L. Skriver, J. Phys. F11, 97 (1981).

I7. The electronic structure of calcium.
J.-P. Jan and H.L. Skriver, J. Phys. F11, 805 (1981).

I8. The s-d transition in compressed lanthanum.
A.K. McMahan, H.L. Skriver, and B. Johansson, Phys. Rev. B23, 5016 (1981).

I9. Electronic structure of the actinide metals.
B. Johansson, H.L. Skriver, and O.K. Andersen, Proc. of the Int. Symp. on "The Physics of Solids under High Pressure", Bad Honnef, Aug. 1981, ed. by J.S. Schilling and R.N. Shelton.

I10. Electronic transitions in praseodymium under pressure.
H.L. Skriver, Proc. of Int. Symp. on "The Physics of Solids under High Pressure", Bad Honnef, Aug 1981, ed. by J.S. Schilling and R.N. Shelton

I11. Calculated structural phase transitions in the alkaline earth metals.
H.L. Skriver, Phys. Rev. Lett. 49, 1768 (1982).

I12. Electronic structure and cohesion in the rare earth metals.
H.L. Skriver in "Systematics and the properties of the lanthanides", ed. by S.P. Sinha (D. Reidel Publ. Co. 1983).

I13. "The LMTO Method".
H.L. Skriver (Springer Verlag, 1984).

I14. Electronic structure and bulk ground state properties of the actinides.
M.S.S. Brooks, B. Johansson, and H.L. Skriver in "Handbook on the physics and chemistry of the actinides" ed. by A.J. Freeman and G.H. Lander (North Holland, 1984).

I15. Crystal structures from one-electron theory.
H.L. Skriver, Phys. Rev. B31, 1909 (1985).

I16. Electron-phonon coupling of the actinide metals.
H.L. Skriver and I. Mertig, submitted to Phys. Rev.

DANSK OVERSIGT

Nærværende afhandling beskriver sammen med de 16 artikler (I1-I16), som er anført i forordet, en serie beregninger af elektroniske tilstande i metalliske grundstoffer samt af nogle af de grundlæggende materialeegenskaber, som baserer sig på disse elektrontilstande. Hele fremstillingen hviler på den lokaltæthedstilnærmelse, der for øjeblikket udgør det mest tilfredsstillende fundament for en eenelektronbeskrivelse af metallers egenskaber. Til gengæld for den enorme reduktion af det tilgrundliggende mangelegemeproblem, som lokaltæthedstilnærmelsen udgør, må eenelektrontilstandene udregnes selvkonsistent i lighed med den "self-consistent field" teknik, man i mange år har anvendt til løsning af atomare problemer. Det selvkonsistente eenelektronproblem er i de foreliggende beregninger løst ved hjælp af en af de såkaldte lineære metoder udviklet af O.K. Andersen og beskrevet i detaljer i bogen "The LMTO Method" (I13).

Det har været et af målene med de foreliggende beregninger at benytte LMTO metoden til at studere, i hvor høj grad lokaltæthedstilnærmelsen giver en korrekt beskrivelse af de metalliske grundstoffers basale materialeegenskaber, som de manifesterer sig eksperimentelt både under normale omstændigheder og under meget høje tryk. Der er medtaget beregninger af egenskaber som volumen (gitterplanafstand, massefylde), bulk modul (sammentrykkelighed), krystalstruktur, spin polarisering (magnetisk moment) og superledende overgangstemperatur. Resultaterne viser, at lokaltæthedstilnærmelsen giver overraskende nøjagtige værdier for disse grundtilstandsegenskaber.

Blandt de grundstoffer, som afhandlingen omhandler, har de lette metaller i aktinideserien, dvs. francium til americium, spillet en central rolle. Båndberegninger fra før 1978 antydede kraftigt, at man her havde en ganske særlig overgangsserie, hvor 5f elektronerne var itinerante i modsætning til for eksempel 4f elektronerne i lanthanideserien. Dette ville betyde, at der måtte forekomme en stigende besætning af 5f båndet allerede fra protaktinium, hvilket var i modstrid med den på daværende tidspunkt accepterede fortolkning af de krystallografiske data. Ifølge denne fortolkning skulle der først forekomme en endelig besætning af 5f tilstande i neptunium eller plutonium, og den anomali i det atomare volumen, som måltes mellem plutonium og americium, skulle stamme fra et valensskift. De lette aktinider blev derfor betragtet som en 6d overgangsserie i lighed med de sædvanlige 3d, 4d og 5d overgangsserier.

De selvkonsistente beregninger af de lette aktiniders atomare volumen og bulk modul (I1,I9,I14) gav et ganske andet billede af årsagerne til aktinide metallernes helt særlige opførsel. Ifølge dette billede udgør de lette aktinider fra thorium til plutonium en 5f overgangsserie, i hvilken 5f båndet gradvist fyldes op med elektroner. Desuden finder der en lokalisering af 5f elektronerne sted mellem plutonium og americium, hvilket giver anledning til den observered anomali i det atomare volumen. Endvidere viste beregningerne, at 5f elektronerne i americium og curium (I5,I9) ville delokalisere under tryk, hvilket senere er blevet eftervist eksperimentelt. Det må retfærdigvis nævnes, at fortolkningen af aktinidernes eksperimentelle kohesive energier kraftigt understøtter ovennævnte billede af årsagerne til aktinidernes opførsel.

I båndberegningerne på aktiniderne skifter grundtilstanden fra at være upolariseret i plutonium til at være spinpolariseret i americium, og det er denne spinpolarisering, der fortolkes som en lokalisering af 5f elektronerne. Da en sådan fortolkning i 1980 ikke var accepteret af alle, var det nærliggende at foretage spinpolariserede beregninger på 3d monooxiderne, idet disse også udviste en anomali i de målte atomare voluminer. Endvidere var det vigtigt, at monooxiderne som funktion af atomnummeret udgjorde standardeksemplet på en metal-isolator overgang, og at den accepterede fortolkning var, at 3d elektronerne lokaliserede mellem VO og MnO, således at de tunge monooxider blev magnetiske isolatorer. De selvkonsistente beregninger (I2) gav nøjagtigt det samme billede af volumenanomalien mellem VO og MnO, som de tidligere havde givet for anomalien mellem plutonium og americium, og styrkede derved ovennævnte billede af aktinideserien. Senere er der udført spinpolariserede beregninger på de lette lanthanider under tryk (I10), og igen finder man, at den spinpolariserede løsning er grundtilstanden i de faser, hvor man eksperimentelt slutter, at 4f elektronerne er lokaliserede.

Chrom er en af de få itinerante antiferromagneter blandt de rene metaller. De to andre er γ-mangan og γ-jern, og da en simpel antiferromagnetisk struktur analog til CsCl-strukturen kan stabiliseres i chrom ved tilsætning af mangan, var det nærliggende at foretage spinpolariserede båndberegninger på denne idealiserede fase. Disse beregninger (I6) gav et rimeligt resultat for delgittermagnetiseringen og for dens trykafhængighed. Nyere og endnu upublicerede beregninger antyder imidlertid, at det antiferromagnetiske moment har været kunstigt stabiliseret i den anvendte model, og at chrom ikke burde have noget moment i den idealiserede fase. Det må dog nævnes i den forbindelse, at en simpel model (I6), som bygger på canonisk båndteori, og som ikke er kunstigt stabiliseret, i det væsentlige giver de samme resultater som de komplette selvkonsistente beregninger. Dette problem er nu under opklaring.

Eksperimenter med Fermifladens trykafhængighed i thorium gav som resultat, at alle de målte ekstremale arealer aftog med stigende tryk, hvilket var i direkte modstrid med den simple betragtning, at det reciprokke gitter udvidede sig under tryk. De selvkonsistente beregninger af Fermifladen i thorium (I3) viste i overensstemmelse med målingerne, at de fleste ekstremale arealer aftog med stigende tryk, og at årsagen til denne usædvanlige trykafhængighed var den trykinducerede overførsel af s elektroner til d båndet. Lignende beregninger er anvendt til at beskrive Fermifladens trykafhængighed i de tunge alkali metaller (I4), idet man dog her måtte justere potentialparametrene, dvs. inkludere ikke lokale effekter, for at få fuld overensstemmelse med eksperimenter.

Man ville umiddelbart forvente at calciums båndstruktur var ret frielektronlignende. DHvA målinger viste imidlertid, at dette ikke var tilfældet, og desuden viste ledningsevnemålinger, at calcium gennemgik en usædvanlig metal-semimetal-metal overgang under stigende tryk. Beregningerne (I7) viste, at disse forhold i store træk kunne beskrives inden for lokaltæthedstilnærmelsen, og at de skyldtes tilstedeværelsen af det ubesatte 3d bånd lige over Ferminiveauet. Det viste sig endvidere, at en detaljeret overensstemmelse med eksperimenter kun kunne opnås ved at justere potentialparametrene i lighed med de justeringer, der blev foretaget under beregningerne på de tunge alkalimetaller.

De fleste lanthanider udviser i deres shockkompressionsdata en anomali, der har været fortolket som et resultatet af enten en overførsel af elektroner fra s til d båndet, et begyndende overlap af xenonskallerne, smeltning, eller delokalisering af 4f elektronerne. De selvkonsistente beregninger (I8) på lanthan under tryk på op til 2 Mbar viste, at afslutningen på s til d overgangen førte til en pludselig stigning i bulkmodulen, og at denne hærdning af gitteret via fononbidraget gav anledning til den målte anomali. Det er derfor nærliggende at slutte, at afslutningen på s til d overgangen også er årsagen til de tilsvarende anomalier fundet i scandium, yttrium og de øvrige sjældne jordarter.

Lanthanidernes kohesive egenskaber er stort set uafhængige af tilstedeværelsen af elektroner i 4f skallen. Faktisk er lanthaniderne samt scandium og yttrium, dvs. de sjældne jordarter, meget ens og kan i henseende til kohesive egenskaber betragtes som 3d, 4d eller 5d overgangsmetaller med omkring to elektroner i d båndet. Her ses bort fra europium og ytterbium, som er divalente og derfor ligner barium. Ovennævnte synsvinkel blev underbygget af de selvkonsistente beregninger (I12) af de sjældne jordarters elektroniske og kohesive egenskaber, idet variationen af det atomare volumen og af kompressibiliteten gennem serien kunne beskrives ved ikke at medtaget 4f tilstandene blandt valenstilstandene, men i stedet behandle dem som atomare niveauer. Kun cerium afviger væsentligt fra dette billede, idet man her kan komme i kontakt med 4f elektronerne ved hjælp af et moderat ydre tryk eller ved at sænke temperaturen. Spinpolariserede beregninger af samme type som tidligere udført på aktiniderne og 3d monooxiderne viste, at grundtilstanden i γ-cerium foruden af sd elektronerne bestod af omtrentlig een spinpolariseret 4f elektron, medens den tilsvarende 4f elektron i α-cerium var upolariseret. Dette resultat underbyggede den fortolkning, at γ-α overgangen i cerium skyldes en delokalisering af 4f elektronen.

Under arbejdet med calcium (I7) blev det klart, at man ved hjælp af den såkaldte kraftformel kunne forklare den systematik, som udvistes af krystalstrukturerne for metallerne i calciumgruppen suppleret med de divalente lanthanider europium og ytterbium. Beregningerne (I11) viste, at disse metallers særlige krystalstruktursekvens, som optrådte både som funktion af atomnummer og som funktion af tryk, skyldtes den inducerede sænkning af det i begyndelsen ubesatte d bånd. Beregningerne førte også til forudsigelsen af adskillige strukturelle faseovergange, hvoraf de fleste var eksperimentelt kendt og en enkelt (fcc→bcc i Ca) senere er blevet påvist.

Resultaterne med metallerne i calciumgruppen gjorde det naturligt at udvide beregningerne til også at omfatte de øvrige metaller i det periodiske system. Dette arbejde (I15), som omfatter ca. 50 metaller, og som udgør hovedparten af nærværende afhandling, viser, at man på grundlag af lokaltæthedstilnærmelsen og ved hjælp af kraftformlen kan beregne, hvilke krystalstrukturer et givet metal ved lav temperatur vil antage som funktion af et eventuelt påtrykt ydre hydrostatisk tryk. Det viser sig desuden, at forekomsten af bestemte krystalstrukturer blandt alkalimetallerne, calciumgruppens metaller og lanthaniderne såvel som blandt de egentlige overgangsmetaller korrelerer med de beregnede d besætningstal. Det er således tilstedeværelsen af et d bånd, som, hvad enten det er besat eller ej, i stor udstrækning er bestemmende for disse metallers krystalstrukturer. Endvidere underbygger beregningerne af ceriums og de lette aktiniders krystalstrukturer billedet af disse grundstoffer som henholdsvis 4f og 5f metaller.

Med resultaterne fra de selvkonsistente beregninger af et givet metals elektronstruktur er man i besiddelse af al den information, som er nødvendig for at bestemme styrken af dette metals elektron-fononkopling. Beregningerne (I16) af koplingsparameteren λ i de lette aktinider viser, at denne er størst i aktinium, og forudsiger en overgangstemperatur på 9 K i dette metal. Beregningerne viser desuden, at λ's variation med atomnummeret tydeligt afspejler den ændring, der finder sted i elektronstrukturen, fra 6d dominans i radium, aktinium og thorium til 5f dominans i protaktinium, uran, neptunium og plutonium. Det er især bemærkelsesværdigt, at df bidraget til elektron-fononkoplingen dør ud i protaktinium, fordi både 6d og 5f båndet er besat. Derved kommer fg bidraget til at dominere elektron-fononkoplingen i de tungere aktinider, dvs. uran til plutonium. I de aktinider, hvor den superledende overgangstemperatur er målt eller skønnet, dvs. thorium til plutonium, er det beregnede λ i god overensstemmelse med de eksperimentelt afledte værdier. I thorium giver en simpel model for fononfrekvensernes volumenafhængighed sammen med beregninger af Hopfieldparameteren en rimelig beskrivelse af den superledende overgangstemperaturs eksperimentelle trykvariation. Man kan derfor udpege en ændring i Fermifladens topologi som årsag til det omslag i overgangstemperaturens trykvariation, som finder sted i området fra 6 til 10 GPa.

ENGLISH RÉSUMÉ

This thesis together with the 16 previously published papers (I1-I16) listed in the preface describes a series of calculations of the electronic states in metallic elements, and of some of the basic properties of metals which can be derived from these electronic states. The presentation is based on the local density approximation which at present forms the most satisfactory foundation for a one-electron description of the properties of metals. In return for the significant reduction of the original many-body problem which the local density approximation brings about, the electronic states must be determined self-consistently in analogy with the "self-consistent field" technique used for atoms. In the present case, the self-consistent electronic-structure problem has been solved by means of one of the linear methods devised by O.K. Andersen and described in detail in "The LMTO Method" (I13).

It has been one of the goals of the present work to establish how well the local density approximation can describe the basic properties of metals as they manifest themselves at normal conditions as well as at elevated pressures. Included are calculations of atomic volume (lattice spacing), bulk modulus (compressibility), crystal structure, spin-polarization (magnetic moment), and superconducting transition temperature. The results show that the local density approximation gives surprisingly accurate values for these ground-state properties.

Among those metals considered in the thesis the light actinides, i.e. francium through americium, have played a most central role. Energy-band calculations from before 1978 strongly suggested that the actinides formed a rather special transition series in which the 5f electrons were itinerant in contrast to, for instance, the 4f electrons in the lanthanides. This would mean an

increasing occupation of the 5f band already from protactinium, which was in contrast to the interpretation of the crystallographic data accepted at that time. According to this interpretation the first finite occupation of 5f states should appear in neptunium or plutonium, and the anomaly in the atomic volume observed between plutonium and americium should be caused by a change of valence. Hence, the light actinides were considered a 6d transition series in analogy to the well-known 3d, 4d, and 5d transition series.

The self-consistent calculations of the atomic volume and bulk modulus of the light actinides (I1,I9,I14) gave a rather different picture of the causes of the special behaviour of the actinides. According to these calculations, the actinides from thorium to plutonium form a 5f transition series in which the 5f band is gradually filled with electrons as the atomic number increases. They, furthermore, imply a localization of the 5f electrons between plutonium and americium resulting in the observed anomaly in the atomic volume. Finally, the calculations showed that the 5f electrons in americium and curium would delocalize under pressure which has been observed experimentally later. It should be mentioned that the interpretation of the observed cohesive energies of the actinides strongly support the above-mentioned picture of these metals.

In the band calculations for the actinides the ground state changes from an unpolarized one in plutonium to a spin-polarized one in americium, and it is this spin-polarization which is interpreted as a localization of the 5f electrons. Such an interpretaion was not accepted by everybody in 1980, and it was therefore natural to perform spin-polarized calculations for the 3d monoxides, since they also exhibited an anomaly in the measured atomic volume. It was, furthermore, important that the series of 3d monoxides were regarded to exhibit the standard example of a metal-insulator transition, and that the accepted interpretation of this phenomenon was that the 3d electrons localized between VO and MnO thus rendering the heavy monoxides magnetic insulators. The self-consistent calculations (I2) gave exactly the same picture of the volume anomaly between VO and MnO as they had given earlier for the anomaly between plutonium and americium and thereby supported the above-mentioned picture of the actinide series.

Chromium is one of the few itinerant antiferromagnets among the elemental metals, the two others being γ-manganese and γ-iron. Since a simple antiferromagnetic structure analogous to the CsCl-structure can be stabilized in chromium by alloying with manganese it was natural to perform spin-polarized calculations for this idealized phase. The calculations (I6) gave reasonable results for the sublattice magnetization and its pressure dependence. However, recent and as yet unpublished calculations suggest that the antiferromagnetic moment has been artificially stabilized within the model and that chromium may be nonmagnetic in the idealized phase. On the other hand, a simple model (I6) which is based on canonical band theory and which is not artificially stabilized gives essentially the same results as the complete self-consistent calculations. This problem is now under investigation.

In the investigation of the pressure dependence of the Fermi surface cross-sections in thorium, one found that all the experimentally observed extremal areas decreased with increasing pressure in contrast to the simple notion that the reciprocal lattice expanded under pressure. The self-consistent calculations (I3) showed in agreement with the measurements that most of the extremal areas decreased with increasing pressure, and that this rather unusual pressure dependence was caused by the pressure-induced transfer of s electrons into the d band. Similar calculations were used to predict the pressure dependence of the Fermi surface of the heavy alkali metals (I4), but in this case one had to adjust the potential parameters, i.e. include non-local effects, in order to obtain complete agreement with experiment.

One might expect the energy bands of calcium to be rather free-electron-like. However, dHvA measurements showed that this was not the case, and in addition electrical resistance measurements indicated that calcium underwent an unusual metal-semimetal-metal transition when subjected to pressure. The calculations (I7) showed that these phenomena could be described within the local density approximation, and that they were caused by the unoccupied 3d band positioned just above the Fermi level. However, a detailed agreement with experiments could only be obtained by adjusting the potential parameters in the manner used in the calculations on the alkali metals mentioned above.

Most of the lanthanides exhibits an anomaly in their shock compression data which has been interpreted as a result of either transfer of electrons from the s band to the d band, a growing overlap of the xenon cores, melting, or a delocalization of the 4f electrons. The self-consistent calculations (I8) on lanthanum in the pressure range up to 200 GPa showed that the termination of the s to d transition caused a sudden stiffening of the lattice and that this gave rise to the measured anomaly via the phonon contribution to the equation of state. It is natural to infer that a similar termination of the s to d transition is also the cause of the corresponding anomalies found in scandium, yttrium, and the other rare earth metals.

The cohesive properties of the lanthanides are to a large degree independent of the presence of electrons in the 4f shell. In fact, the rare earths, i.e. scandium, yttrium, and the lanthanides, have similar cohesive properties and may in this respect be regarded as 3d, 4d, or 5d transition metals with approximately two electrons in the d band. Here we exclude europium and ytterbium which are divalent and therefore resemble barium. The above viewpoint was supported by the self-consistent calculations (I12) which showed that the variation of the atomic volume and the bulk modulus through the series could be explained by including the 4f electrons in the core. Only cerium deviates from this picture because here one may get in touch with the 4f electron by applying a moderate pressure or by lowering the temperature. Spin-polarized calculations similar to those performed earlier for the actinides and the 3d monoxides showed that the ground state in γ-cerium in addition to the sd electrons consisted of approximately one spin-polarized 4f electron while the corresponding 4f electron in α-cerium was unpolarized. This result supported the interpretation of the γ-α transition in cerium as the result of a delocalization of the 4f electron.

During the work on calcium (I7) it became clear that the so-called force relation could be used to explain the systematics exhibited by the crystal structures of the alkaline earth metals and the two divalent lanthanides europium and ytterbium. The calculations (I11) showed that the particular crystal structure sequence found among these metals as a function of both atomic number and applied pressure was caused by the induced lowering of the initally unoccupied d band. Futhermore, the calculations predicted several structural phase transitions of which several were experimentally known. One of the transitions (fcc→bcc in Ca) unobserved at the time of the calculation has later been confirmed experimentally.

With the results of the calculations on the alkaline earth metals in mind it was natural to extend the treatment to include most of the other metals in the periodic table. This work (I15), which includes approximately 50 metals and which forms the main part of the present thesis, shows that the local density approximation in conjunction with the force relation may be used to calculate which crystal structure a given metal at low temperatures will take up as a function of an applied external pressure. It further shows that the appearance of certain crystal structure sequences among the alkali metal, the alkaline earth metals and the lanthanides as well as the proper transition metals correlates with the calculated d occupation numbers. Hence, it is the presence of a d band, whether occupied or not, which to a large extent determines the crystal structures of these metals. Furthermore, the calculations of the crystal structures of cerium and the light actinides support the picture of these element as 4f and 5f metals, respectively.

The results of the self-consistent calculations of the electronic structure of a given metal include all the information needed to estimate the strength of its electron-phonon coupling. In the calculations (I16) for the light actinides it is found that the coupling parameter λ reaches its maximum value in actinium, and a transition temperature of 9 K is predicted for this metal. It is furthermore found that the variation in λ with atomic number, clearly reflects the changes, which occur in the electronic structure, from a 6d-dominated behaviour in radium, actinium, and thorium to a 5f-dominated situation in protactinium, uranium, neptunium, and plutonium. It is particularly noteworthy that the df contribution vanishes in protactinium because the 6d and the 5f bands are simultaneously occupied. Thereby, the electron-phonon coupling in the heavier actinides, i.e. uranium through plutonium, becomes dominated by the fg contribution. In those actinides where the superconducting transition temperature is measured or estimated, i.e. thorium through plutonium, the calculated λ is in good agreement with the experimentally derived values. In thorium a simple model for the volume dependence of the phonon frequencies in conjunction with the calculations of the Hopfield parameter gives a reasonable description of the measured variation of the transition temperature with applied pressure. It is thus possible to connect the pronounced change in the pressure variation of the transition temperature, which occurs in the range from 6 to 10 GPA, with a change in the topology of the Fermi surface.

1. INTRODUCTION

Many of the characteristic properties of the metallic elements are a consequence of their ability at normal temperature and pressure to form crystals in which the metal atoms are arranged in a regular pattern which repeats itself throughout the interior of the crystal. These crystals are the microscopic building blocks of all the pieces of metal which we encounter around us, and it is therefore of great importance to investigate their basic properties both experimentally and theoretically. The hope is of course that by isolating and understanding the factors that govern the stability of the cystal structures found in nature one may eventually be able to design metals with specified properties.

The crystal structures of solid state materials are established by X-ray diffraction experiments, and the results for the elemental metals are compiled in Fig. 1. It turns out that the variety of crystal structures which the metallic elements take on is limited to essentially the five types shown on Fig. 2, and that four of these five structures are so-called close-packed structures. The term close-packed refers to the fact that the fcc, hcp, dhcp, and Sm-type structures can be derived from stacking hexagonal layers of spheres of equal radii in the closest possible fashion. As a result of this close-packing the coordination number in these four structures is 12, each atom being surrounded by 12 nearest neighbours. The bcc structure is a little less close-packed and has a coordination number of 8, although it is sometimes referred to as having a coordination number of 14 on account of the 6 next nearest neighbours, which are only slightly farther away than the nearest neighbours.

0.0 - 0.8		1	2	3.5	5	6	7	8.5	9.5	10	n_d
Li hcp	Be hcp										
Na hcp	Mg hcp										
K bcc	Ca fcc	Sc hcp	Ti hcp	V bcc	Cr bcc	Mn (bcc)	Fe bcc	Co hcp	Ni fcc	Cu fcc	Zn hcp
Rb bcc	Sr fcc	Y hcp	Zr hcp	Nb bcc	Mo bcc	Tc hcp	Ru hcp	Rh fcc	Pd fcc	Ag fcc	Cd hcp
Cs bcc	Ba bcc	Lu hcp	Hf hcp	Ta bcc	W bcc	Re hcp	Os hcp	Ir fcc	Pt fcc	Au fcc	Hg (fcc)
Fr	Ra bcc										

La dhcp	Ce fcc	Pr dhcp	Nd dhcp	Pm dhcp	Sm Sm-t	Eu bcc	Gd hcp	Tb hcp	Dy hcp	Ho hcp	Er hcp	Tm hcp	Yb hcp
Th fcc	Pa bct	U orth.	Np orth.	Pu mon.	Am dhcp	Cm dhcp	Bk dhcp	Cf dhcp	Es	Fm	Md	No	Lr

Fig. 1. Crystal structures of the metallic elements at low temperature.

It may be seen from Fig. 1 that the crystal structures of the metallic elements tend to occur in sequences when viewed as functions of atomic number or hydrostatic pressure. The most prominent example of this phenomenon occurs with the d transition metals, where all three transition series, excluding the four magnetic 3d metals, exihibit the same hcp→bcc→hcp→fcc sequence as the d states become progressively filled. A similar sequence is found in the lanthanides where the hcp→Sm-type→ dhcp→fcc sequence established as a function of decreasing atomic number may also be realized by subjecting each individual lanthanide metal, except Ce, Eu, and Yb, to hydrostatic pressure. Finally, the alkaline earth metals, together with the divalent rare earths Eu and Yb, are part of a short fcc→bcc sequence which is also realized in Ca, Sr, and Yb under high pressure.

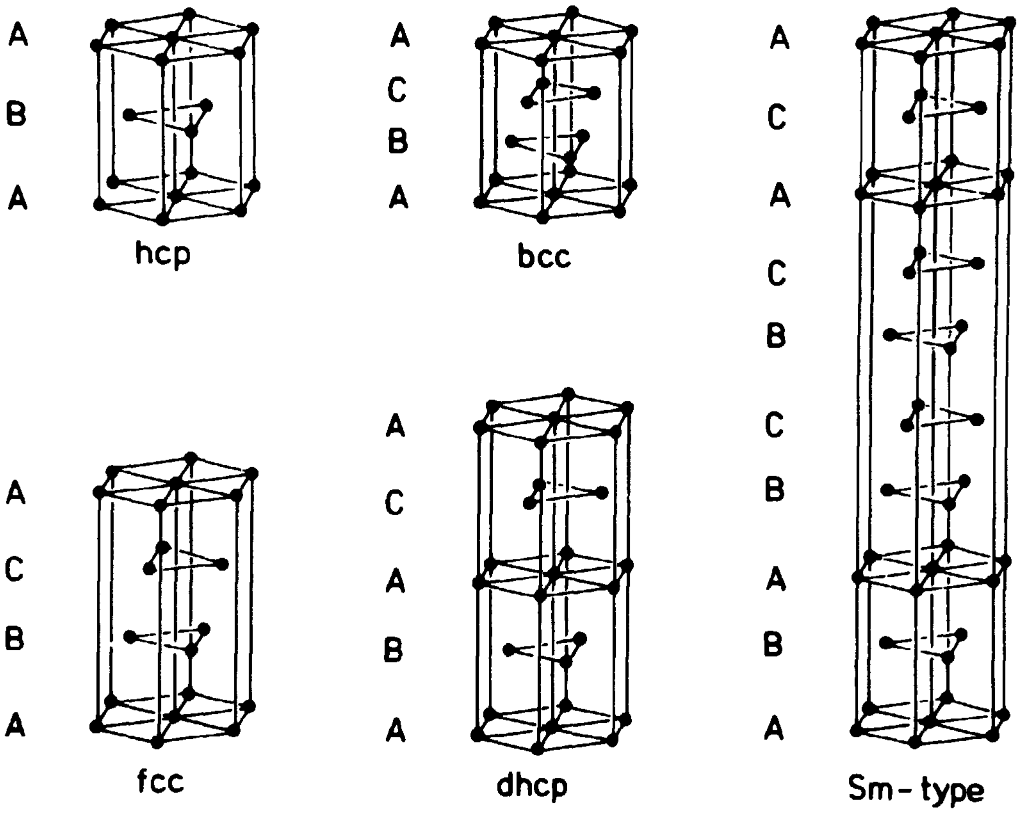

Fig. 2. Close-packed crystal structures of the elemental metals.

In the present contribution we shall establish the extent to which the systematics outlined above can be explained by means of a state-of-the-art theory for the ground state of the bonding electrons. The theory we apply is a one-electron theory in which each electron is treated as an independent particle moving in the effective potential from all the other electrons and the nuclei, and the only input to the calculations is the atomic number of the metal to be treated. In order to be able to reduce the original many-body problem significantly one has to solve the electronic structure problem self-consistently, and to this end we use the Linear Muffin-Tin Orbital (LMTO) method (Andersen 1975) in conjunction with a scaling principle as outlined by Skriver (1984).

The structural energy differences which determine the relative stability of the crystal structures to be studied are in turn obtained from the one-electron states by means of Andersen's force theorem (Mackintosh and Andersen 1980). The whole procedure is quite general and allows us to treat all metals on the same footing.

The remainder of the present contribution is organized as follows: In Sect. 1.1 we outline the simplest possible theory of structural stability in terms of the density of electronic states, and in the following section 1.2 we apply this simple theory to state densities obtained by means of canonical band theory. In Sect. 2 we review previous theoretical efforts in the field and compare them with the present approach, the theoretical foundations of which are discussed in Sect. 3. In Sect. 4 we outline an electrostatic correction to the Atomic Sphere Approximation (ASA) which becomes important for structures less close-packed than those shown in Fig. 2. Finally, in Sect. 5 we present the calculated structural energy differences for the alkalis, the alkaline earths, the transition metals, the lanthanides, and the light actinides.

1.1. A simple theory of structural stability

In the main part of the following we shall describe the results of a series of calculations of the relative stability of the crystal structures of some 40 elemental metals. In such a presentation, centred around an account of theoretical results and their relation to experimental observations, it is easy to lose track of the principles upon which the calculations are based. We shall therefore immediately present a simple model which will illustrate these principles and in addition will serve to make more comprehensible the complete calculations to be described later.

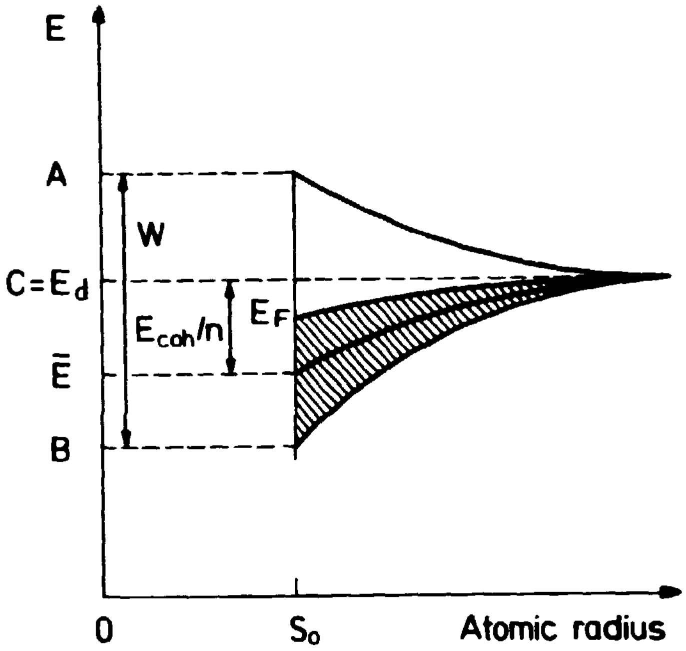

Fig. 3. Formation of the energy band of a metal from an atomic energy E_d. The width is W, the bottom and top B and A, respectively, the Fermi level, i.e. the highest occupied energy E_F, the cohesive energy E_{coh}, and the number of electrons per atom n.

According to standard textbooks one may imagine a metal formed in the thought experiment illustrated in Fig. 3 where N initially infinitely separated metal atoms are slowly brought together. Here we shall consider specifically a transition metal in which the important states have d character. As a result of the increasing contact between neighbouring atoms the 5N atomic d states give rise to a band of energies ranging from B which corresponds to bonding between most neighbours to A which corresponds to antibonding between them. The band of energies formed in this way constitutes the energy band of the metal, and it contains all the one-electron states which the conduction electrons may occupy.

The energy gained in the above process is called the cohesive energy, and according to Fig. 3 it is simply the difference between the total atomic energy nE_d and the total band energy

$n\bar{E}$, i.e.

$$E_{coh} = n(E_d - \bar{E}) \qquad (1)$$

assuming an occupation of n d electrons per atom. In writing down (1) we have furthermore assumed that the d states broader around the atomic level E_d, that is that the centre C of the d band coincides with E_d.

The average energy $\bar{E}$, which corresponds to the centre of gravity of the occupied part of the d band and which enters (1), may be obtained by summing the one-electron energies ε_i between the bottom of the band B and the highest occupied one-electron level E_F, i.e.

$$\begin{aligned} \bar{E} &= n^{-1} \sum_i^{occ} \varepsilon_i \\ &= n^{-1} \int^{E_F} EN(E)dE \end{aligned} \qquad (2)$$

where we have introduced the state density function N(E) which describes how the states are distributed in the energy range from B to A.

If we assume that all states within the d band are equally probable the state density will have the rectangular shape shown in Fig. 4a, and the cohesive energy will simply be given by

$$E^r_{coh} = \frac{W}{20} n(10-n) \qquad (3)$$

As noted by Friedel (1969) this form clearly exhibits the parabolic variation with the d occupation, cf. Fig. 4c, which is also found experimentally (Gschneidner 1969, Friedel and Sayers 1977), especially when proper account is taken of the atomic effects (Brooks and Johansson 1983), and this agreement was taken as confirmation of the assumptions of the model outlined above.

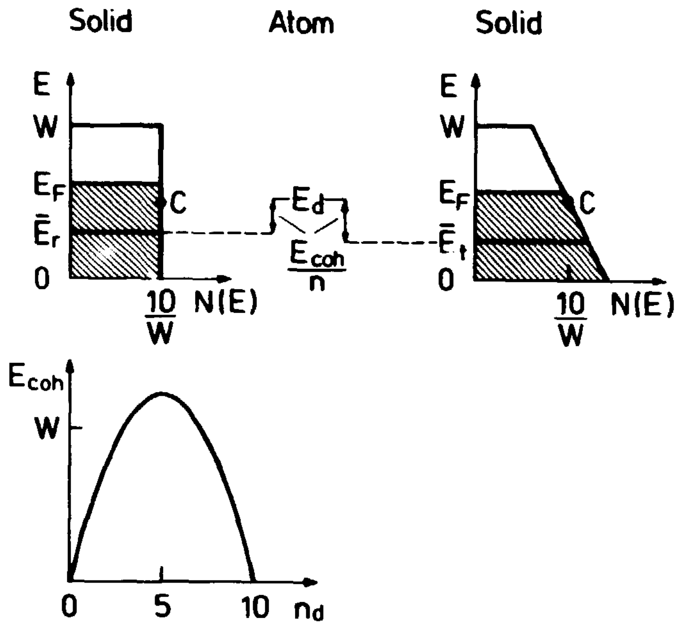

Fig. 4. Rectangular a) and skew b) state densities modelling the dependence of the cohesive energy upon crystal structure. The cohesive energy as a function of d occupation n for the rectangular state density is labelled c).

From Eq.(1) and Fig. 4 it is clear that the energy gained in forming a metal from the free atoms depends upon the relative position of the atomic d level E_d and the average band energy $\bar{E}$. The latter depends upon the shape of the state density which in turn depends upon the arrangement of the atoms in the metal crystal, and hence different crystal structures will lead to different cohesive energies.

It follows that the relative stability of all possible crystal structures for a given metal will be determined by the particular shape of the corresponding state densities. We have illustrated this simple result in Fig. 4 from which it is straightforward to see that the crystal structure leading to the skew state density b) will have a higher cohesive energy and hence be more stable than the structure which leads to the rectangular state density a) on account of the lowering of $\bar{E}$. Hence, the relative stability of two crystal structures may be estimated simply by comparing the corresponding average band energies $\bar{E}$.

In the complete calculations to be reported later we have applied this simple principle to accurately calculated state densities, and the success with which the results explain the experimental observations may be taken as a justification of the assumptions underlying the one-electron approach outlined above. As will be explained in Sect. 3 there is however also theoretical justification for such a one-electron approach in the form of the so-called force theorem (Mackintosh and Andersen 1980) which dictates how the band structures and the corresponding state densities of the metals in the different crystal structures should be calculated.

1.2. Structural stability from canonical band theory

The concept of canonical bands (Andersen 1975, Andersen and Jepsen 1977) gives rise to a simple and yet realistic procedure for estimating the relative stability of the close-packed crystal structures which form for instance the transition metal sequence, Fig. 1. According to canonical band theory an unhybridized, pure ℓ band may be obtained from (Andersen and Jepsen 1977, Skriver 1984)

$$E_{\ell i}(\underline{k}) = C_\ell + \frac{1}{\mu_\ell S^2} \frac{\mathcal{S}^{k}_{\ell i}}{1-\gamma_\ell \mathcal{S}^{k}_{\ell i}} \qquad (4)$$

where $\mathcal{S}^{k}_{\ell i}$ are the canonical bands which depend solely upon the crystal structure, S is the atomic Wigner-Seitz radius, C_ℓ the center of the ℓ band, μ_ℓ the band mass, and γ_ℓ a distortion parameter. The three potential parameters C_ℓ, μ_ℓ and γ_ℓ depend upon potential and volume but not upon crystal structure.

In a transition metal one may to a good approximation neglect all but the d bands. Since furthermore γ_d is small, one has the following potential-, i.e. atomic number-, independent estimate of the band contribution to the cohesive energy E_{coh}

$$\begin{aligned} \mu_d\, S^2\, E_{coh} &= -\mu_d S^2 \int^{E_F} (E - C_d)\, N_d(E)\, dE \\ &= -\int^{\mathcal{S}_d(n_d)} \mathcal{S}_d\, \tilde{N}_d(\mathcal{S}_d)\, d\mathcal{S}_d \end{aligned} \qquad (5)$$

in terms of the first-order moment of the canonical state density $\tilde{N}_d$. Andersen et al. (1977) have evaluated (5) as a function of d occupation number n_d and found the expected parabolic behaviour (Friedel 1969) which may also be obtained directly if $N_d(E)$ is approximated by a rectangular state density as explained in the introduction.

Since the center C_d and the band mass μ_d are independent of crystal structure, the first-order moment (5) may be used to estimate the structural energy differences according to Eq. (9). The result shown in Fig. 5 is identical to that of Andersen et al. (1977) and similar to the one obtained by Pettifor (1970). It accounts qualitatively for the crystal structures of the non-magnetic transition metals, Fig. 1, in the beginning of the series but fails to predict the fcc structure at high d occupations. This failure is attributed either to a failure of the force relation (Mackintosh and Andersen 1980) or to hard-core effects (Pettifor 1970, 1972, 1977) omitted in Eq. (5).

The lanthanide metals are found to have d occupation numbers varying almost linearly with atomic number from 1.99 in La to 1.45 in Lu (Skriver 1983) or from 2.5 to 2.0 if hybridization is neglected (Duthie and Pettifor 1977). Furthermore, their crystal structures are as closely packed as are those of the d transition metals and hence their structural energy differences may be estimated by Eq. (5). The results shown in Fig. 6 are

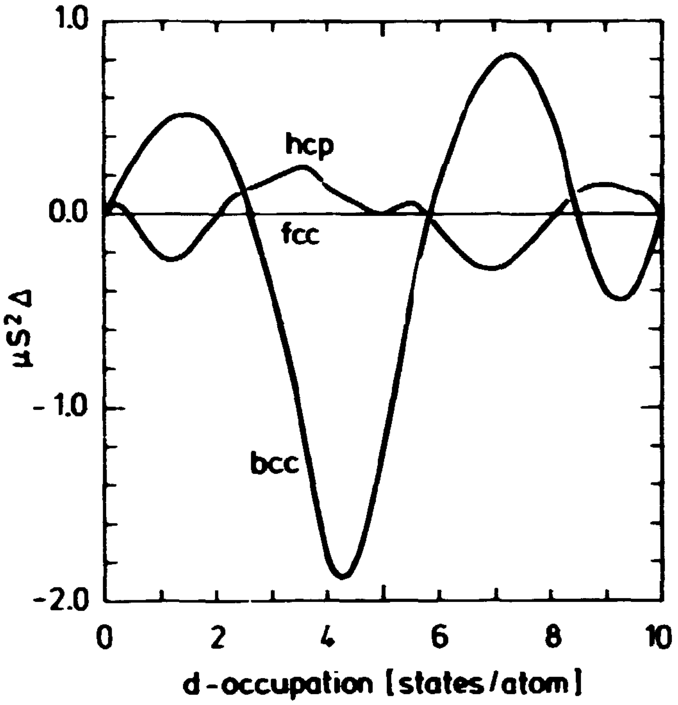

Fig. 5. Structural energy differences obtained from canonical d bands by means of Eq. (5) as functions of the calculated canonical d occupation.

qualitatively similar to but on the average a factor 1.7 smaller than those obtained by Duthie and Pettifor (1977). In this comparison one may take the d-band width to be approximately $25/\mu_d S^2$ in order to bring their Fig. 2 onto the scale of Fig. 6. The results in Fig. 6 account qualitatively for the hcp→Sm-type→dhcp sequence found experimentally in going from Lu to La and more importantly perhaps, since the d occupation for the lanthanides is calculated to increase with pressure and decrease with atomic number, they also explain that part of the same sequence is realized when a particular lanthanide metal is subjected to pressure. It therefore follows that the d-occupation number, which is essentially a measure of the relative position of the s and d bands, may be used to rationalize the structure of the generalized phase diagram for the lanthanides constructed by Johansson and Rosengren (1975).

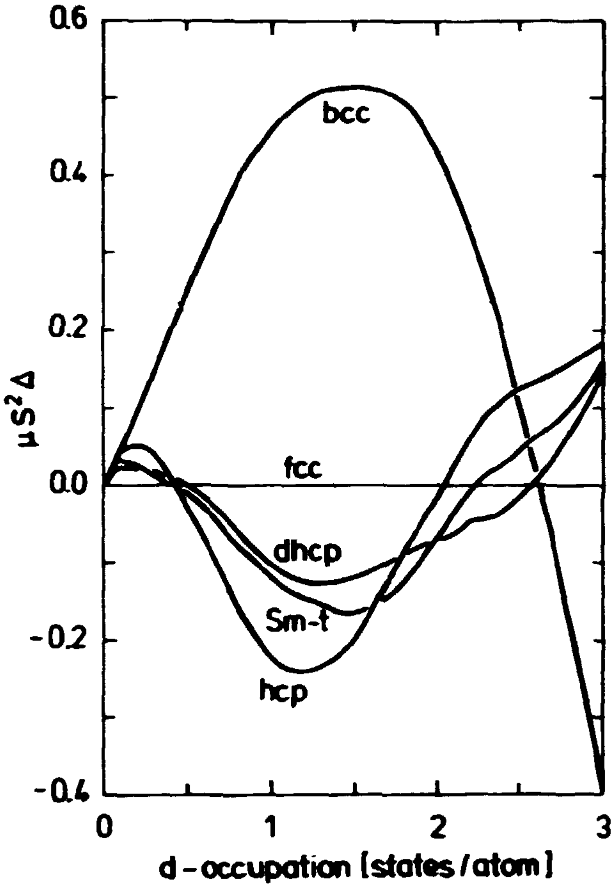

Fig. 6. Structural energy differences obtained from canonical d bands by means of Eq. (5) in the d occupation number range appropriate to the lanthanide crystal structure sequence.

At the present stage one should realize that the results obtained by canonical band theory and shown in Figs. 5 and 6 are only qualitative. Indeed, if one considers Fig. 7 where the canonical estimates are compared with experimental crystal structures, one finds that the canonical theory in several cases does not predict the correct crystal structure independently of whether one uses the self-consistent d-occupation numbers or those obtained conventionally by nonlinear interpolation along a row in the periodic table (see Fig. 1). La, Re, and Ir, for instance,

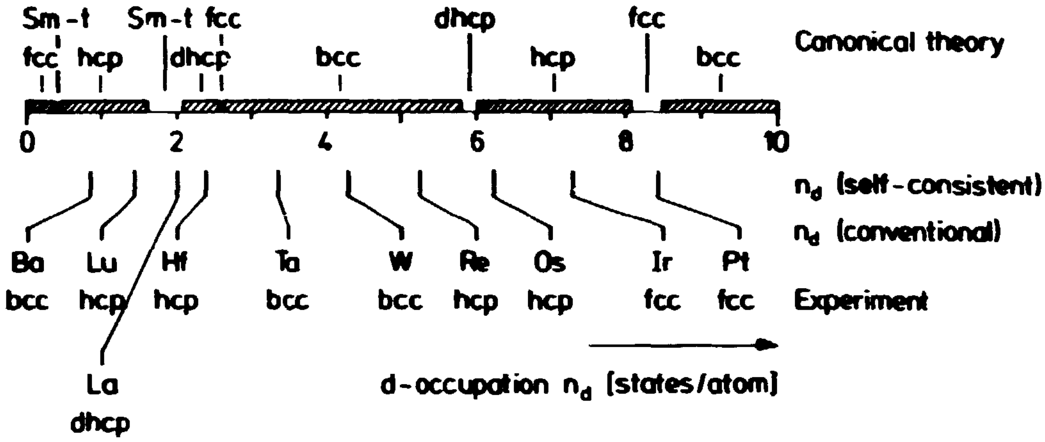

Fig. 7. Canonical estimate of the most stable close-packed crystal structure as a function of the calculated d occupation number compiled from Figs. 2 & 3, horizontal bars. Below are given two estimates of the actual d occupation numbers of the 5d metals together with the experimentally observed crystal structures.

are examples of incorrect predictions, but here one may argue that the correct crystal structure is nearby and hence the failure of the theory may be considered less important. Ba is another example and in this case there is no nearby bcc structure. However, in Ba the d-occupation number is only a fraction of the total number of electrons and hence a theory based solely upon unhybridized d bands is probably inapplicable. The most important failure is connected with the d occupation range from 1.6 to 2.6 [states/atom]. According to Fig. 7, La, Pr, Nd, and Pm should incorrectly form in the Sm-type structure while Ti, Zr, and Hf are expected to be part of the lanthanide sequence. Instead, the latter three metals form in the hcp structure which is the least stable among those considered in the d occupation range above 2 [states/atom].

It may be concluded that the simple estimate of structural energy differences obtained by means of the first-order moments of the canonical state densities is of limited value as a predictive tool. It is, however, of sufficient physical significance to warrant a study of the crystal structure of metals using a more accurate one-electron theory, and to be used in the interpretation of the results of such a study.

2. THEORETICAL APPROACHES TO STRUCTURAL STABILITY

The most prominent crystal structure sequence in the periodic table is the hcp→bcc→hcp→fcc sequence found among the d transition metals, see Fig. 1. Qualitative explanations of this trend have been given by Brewer (1967) in terms of Engel correlations between the valence sp electrons and by Kaufman and Bernstein (1970) in terms of semi-empirical thermodynamic calculations of phase diagrams, whereas Deegan (1968), Dalton and Deegan (1969), and Ducastelle and Cyrot-Lackmann (1971) have attempted more quantitative approaches based upon one-electron theory.

Deegan (1968) and Dalton and Deegan (1969) showed that the stability of the bcc phase for nearly half-filled d shells might be explained by differences in the sum of one-electron band structure energies, and they pointed to the special double-peak structure of a bcc state density as responsible for this stability. Later, Pettifor (1970, 1972) extended the work of Dalton and Deegan and showed that the entire crystal-structure sequence of the transition metals could be accounted for by a one-electron approach. In his calculations Pettifor (1977) found no evidence for the Brewer-Engel correlation (Brewer 1967), which relates crystal structure stability to the sp occupation numbers, and instead he related the hcp→bcc→hcp→fcc sequence to the change in d occupation which takes place across a transition series. This latter viewpoint has proven to be very fruitful in that it may be used as a simple "one-parameter theory" which in many cases provides remarkably good estimates of structural stabilities also for non-transition metals such as the alkaline earths (Skriver 1982).

The crystal structures of the trivalent lanthanides, i.e. Pr through Lu except Eu and Yb, exhibit such regularity, as functions of atomic number, pressure, and temperature, that Johansson and Rosengren (1975) were able to construct a single generalized phase diagram for these metals. In this case the crystal structures observed under ambient conditions, (see e.g., Beaudry 1978) are found to be part of the sequence hcp→Sm-type→dhcp→fcc→ fcc′ established by high-pressure experiments (Jayaraman and Sherwood 1964, Piermarini and Weir 1964, Jayaraman 1965, McWhan and Stevens 1965, 1967, Liu et al. 1973, Liu 1975, Nakaue 1978) and alloying (Koch 1970). Here fcc′ refers to the recently discovered distorted fcc structure (Grosshans et al. 1981). The lanthanide sequence is also found in Y (Vohra et al. 1981) where there are no occupied f states and in the heavier actinide (Stephens et al. 1968, Akella et al. 1979, 1980, Roof et al. 1980, Roof 1982, Benedict et al. 1984) at pressures where the 5f states are still localized. Qualitative explanations of the hcp→Sm-type→dhcp→fcc sequence have been attempted in terms of pseudopotential theory by Hodges (1967) and in terms of a 4f contribution to the bonding by Gschneidner and Valletta (1968), while Duthie and Pettifor (1977) gave a quantitative explanation in terms of one-electron theory.

Duthie and Pettifor (1977) showed that the lanthanide crystal-structure sequence could be explained by differences in the total one-electron band-structure energies, and they found a strong correlation between crystal structure and d-occupation number. Hence it appears that the lanthanide metals, as far as their crystal structures are concerned, behave as ordinary 5d transition metals with a d-occupation ranging from approximately 2.0 in La to 1.5 in Lu. This result is very appealing because there is a one-to-one correspondence between the calculated d-occupation number and the single f parameter used by Johansson and Rosengren (1975) and Johansson (1978) to rationalize the lanthanide crystal-structure sequence, and because it is immediately possible to understand the behaviour of Y (Vohra et al. 1981) and the heavy actinides (Stepnens et al. 1968, Akella et al. 1979, 1980, Roof et al. 1980, Roof 1982, Benedict et al. 1984) within the same framework.

At first sight it may seem surprising that the crystal structures of so many metals can be explained on the basis of differences in the total one-electron band-structure energies alone, since the total electronic energy, apart from the one-electron term, has contributions also from double counting and exchange-correlation. However, it has recently been shown (Andersen et al., 1979, Mackintosh and Andersen 1980, see also page 119 of Heine 1980) that, provided the one-electron potential is kept frozen upon a displacement of the atoms, the corresponding changes in the double counting and exchange-correlation terms cancel to first order in the appropriate local electron density, and hence the difference in the sum of the one-electron energies, obtained by means of the frozen, i.e. not self-consistently relaxed, potential, will give an accurate estimate of the corresponding self-consistent change in the total electronic energy. It is exactly this cancellation, which also leads to the so-called pressure expression (Nieminen and Hodges 1976, Pettifor 1976) and to the more general force relation derived by Andersen (see Mackintosh and Andersen 1980), that in turn justifies the simple band structure approach taken for instance by Pettifor (1970, 1972, 1977).

In their work Pettifor (1970, 1972, 1977) and Duthie and Pettifor (1977) focused their attention on the contribution to the total energy from the d bands and either neglected hybridization with the sp bands entirely or included hybridization appropriate to some average element. Hence their picture is essentially a canonical one (cf. Sect. 1.2) in which the energy band structures depend only upon crystal structure and not upon band-filling. It is obvious that such a picture, although adequate for the d transition metals, will fail in cases where states of non d character are as or more important than the d states, as they are for instance in the alkali, the alkaline earth and light actinide metals. Fortunately, the force theorem is not restricted to the canonical approximation and it has recently been used in theoretical investigations of crystal structures in the third row metals (Moriarty and McMahan 1982, McMahan and Moriarty 1983) the alkaline earth metals (Skriver 1982), and in Cs above the s-d transition (McMahan 1984).

In the present work we go beyond the canonical approximation and use the force theorem (Mackintosh and Andersen 1980) to calculate the structural energy differences for all the 3d, 4d, and 5d transition metals at zero pressure and temperature. In addition we investigate the effect of hydrostatic pressure upon the crystal structures of alkali, alkaline earth, lanthanide and actinide metals.

Traditionally the non-transition metals, e.g. alkali and alkaline earth metals, have been treated by means of pseudopotential theory, and the crystal structures predicted from this approach are generally in good agreement with experiment (Animalu 1967, Heine and Weaire 1970, Moriarty 1973, 1982, Hafner and Heine 1983, Young and Ross 1984). It has, however, not been straightforward to generalize the pseudopotential method to treat narrow d-band materials, and to do so one has had to add localized orbitals to the plane-wave basis (Zunger and Cohen 1979). Thus the d band in K is described by the d component of plane waves while that of Cu is described by additional d orbitals, which is somewhat inconsistent with the smooth lowering of the 3d band through the series K, Ca, Sc, ..., Cu. The method has, however, proved to be very accurate.

The present approach, based upon the Linear Muffin-Tin Orbital (LMTO) method (Andersen 1975), has the advantage of employing the same type of basis functions for all the elements thus leading to a conceptually consistent description of trends throughout the periodic table. In addition, the LMTO method is extremely efficient on a computer requiring only the solution of an eigenvalue problem of 9×9 (or 16×16 if f states are included) per atom at each point in reciprocal space. Since we are mainly interested in trends, we have neglected the nonspherical contributions to the charge density, which may explain what seems to be a systematic overestimate of the calculated structural energy differences. We have furthermore neglected a structure-dependent electrostatic interaction between atomic spheres except in the few cases where it contributes significantly to the energy differences.

3. ONE-ELECTRON THEORY OF STRUCTURAL STABILITY

At low temperatures the crystal structure of a metal is determined by the total electronic energy U in addition to a small contribution from the zero-point motion*), which we shall neglect. Hence, if one wants to determine the stability of some crystal structure, say bcc, against some reference structure, which we shall take to be the close-packed fcc structure, one may calculate the total energy of both phases and form the structural energy difference

$$\Delta_{bcc-fcc} = U_{bcc} - U_{fcc} \tag{6}$$

---

*) The zero-point energy is proportional to the Debye temperature i.e. $E_O = (9/8)\ k_B\ \Theta_D$. Typically Θ_D varies by 1-10 [K] between different structures of the same metal (see Gschneidner 1964) and hence the ΔE_O to be added to (6) is of the order of 0.01-0.1 [mRy] which in most cases will be too small to affect the structural stabilities.

where the total energy according to the local density approximation (Kohn and Sham 1965) may be written as the sum over occupied states of the one-electron energies ε_i corrected for double counting, plus electrostatic terms (see e.g., sections 13 and 15 of Heine 1980 or sections 7.2 and 7.3 of Skriver 1984), i.e.

$$U = \sum_{i}^{occ} \varepsilon_i \; - \text{ double counting } + \text{ electrostatic} \qquad (7)$$

If the difference (6) is negative the bcc structure will be stable against fcc.

The total energy for say a 4d metal is of the order of 10^4 [Ry] mainly because of the contributions from the low-lying core levels while typical structural energy differences are of the order of 10^{-3} [Ry]. Hence, extreme accuracy is needed in order to use (6) directly, and one would like to have a numerically more satisfactory procedure. The force theorem (Mackintosh and Andersen 1980) gives rise to such a procedure, but more importantly perhaps it casts the problem of finding stable crystal structures into a form where the significant contribution comes from the one-electron valence energies and not from double counting nor from the deep core-levels.

The force theorem dictates that we adopt the following procedure: For a given metal at a given atomic volume one must solve the energy-band problem self-consistently assuming the reference crystal structure. To this end we use the LMTO method (Andersen 1975) within the Atomic Sphere Approximation (ASA) including the combined correction to the ASA (Andersen 1975). In addition we take account of the relativistic effects, except spin-orbit coupling which we neglect, include exchange-correlation in the form given by von Barth and Hedin (1972), and freeze the appropriate cores. This part of the calculations is described in detail by Skriver (1984). We have now minimized the energy functional U{n} with respect to changes in the electron density n and obtained the ground state density n_{fcc}^{sc}. Because of the stationary properties of U one may obtain, for instance, U_{bcc} from a trial charge-density n_{bcc}^{tr} constructed by positioning the self-consistent fcc atomic-sphere potentials in a bcc geometry, solving the one-electron Schrödinger equation, and populating the lowest-lying one-electron states. Hence,

$$\Delta_{bcc-fcc} = U_{bcc}\left\{n_{bcc}^{tr}\right\} - U_{fcc}\left\{n_{fcc}^{sc}\right\} \tag{8}$$

where the errors relative to (6) are of second order in $n_{bcc}^{tr} - n_{bcc}^{sc}$. Now, the use of a frozen, i.e. not self-consistently relaxed, potential to generate n_{bcc}^{tr} ensures that the chemical shifts in the core levels drop out of Eq. (8) and also that the double-counting terms cancel. Hence, the core level energies and the double-counting terms may be neglected entirely in Eq. (7) leaving only the valence one-electron energies and the electrostatic terms to be considered. The fact that the freezing of the potential leads to such a computationally simple and conceptually important result was already noted by Pettifor (1976) in his derivation of the pressure expression.

Within the atomic sphere approximation (Andersen 1975) the atomic Wigner-Seitz sphere of an elemental metal is neutral and there is therefore no electrostatic interaction between the spheres. Hence the electrostatic terms in Eq. (7) vanish and the structural energy difference (8) may be obtained from

$$\Delta_{bcc-fcc} = \int^{E_F} E\, N_{bcc}(E)\, dE - \int^{E_F} E\, N_{fcc}(E)\, dE \tag{9}$$

where N(E) is the one-electron state density. Furthermore, the ASA allows a separation of the potential- and crystal-structure-dependent parts of the energy band problem (Andersen 1975, Andersen and Jepsen 1977, Skriver 1984). Hence, all that is required at a given atomic volume, in addition to the self-consistent fcc calculation, is to calculate the energy bands of the relevant crystal structures with the use of the self-consistent fcc potential parameters, evaluate the sums of the one-electron energies, and subtract according to Eq. (9). This procedure is quite general, treats all s, p, d, and f electrons on the same footing, and may be applied to all metals in the periodic table.

4. MADELUNG CORRECTION TO THE ASA

The errors of neglecting the structure-dependent electrostatic terms in (7) may be estimated by means of what has been called either the Muffin-Tin (Glötzel and Andersen, unpublished) or Ewald (Esposito et al. 1980) correction to the ASA. To derive this correction one observes that the electrostatic energy per ion of a lattice of point ions of charge $q_S|e|$ embedded in a negative neutralizing uniform charge density is given by the well-known Madelung expression

$$U_M = - 1/2(q_S|e|)^2 \frac{\alpha_M}{S} \tag{10}$$

where α_M is the lattice Madelung constant and S the atomic Wigner-Seitz radius. In the ASA this expression is approximated by the energy of an ion embedded in a single neutralizing atomic sphere, whereby $\alpha_M(\text{ASA}) = 1.8$. The correction is therefore

$$\Delta U_M = 1/2(q_S|e|)^2 \frac{1.8-\alpha_M}{S} \tag{11}$$

In a Muffin-Tin model the effective charge $q_S|e|$ is the charge density in the interstitial region between the Muffin-Tin spheres times the volume of the unit cell. In the ASA this becomes

Table 1. Madelung constant to be used in Eq. (11).

	α_M	$1.8-\alpha_M$		$(1.8-\alpha_M)-(\,)_{fcc}$	
fcc	1.79174723	8.253	10^{-3}		
bcc	1.79185851	8.142	10^{-3}	-0.111	10^{-3}
hcp	1.79167624	8.324	10^{-3}	0.071	10^{-3}
α-U*)	1.78418298	15.817	10^{-3}	7.564	10^{-3}

*) b/a = 1.964, c/a = 1.709, y = 0.1

$$q_s |e| = \frac{4\pi}{3} S^3 n(S) |e| \tag{12}$$

where n(S) is the electron density at the atomic radius.

For close-packed crystal structures α_M is approximately 1.8, see Table 1, and hence the correction (11) is smallest in these. Typically q_s^2/S lies in the range from 0.5 to 5 [a.u.] so that the Madelung correction for the bcc and hcp structures relative to the fcc structure lies in the range 0.05 to 0.5 [mRy].

5. STRUCTURAL STABILITY FROM LMTO BAND CALCULATIONS

In the following we shall present structural energy differences for most metallic elements to the left of and including the noble metals as obtained by means of the procedure described in Sect. 3. The results will be valid only at low temperature and at atomospheric pressure, strictly T = 0 [K] and P = 0 [GPa], except in a few important cases where structural stability has been followed as a function of pressure.

5.1. The alkali metals

The calculated structural energy differences for alkali metals at equilibrium are almost two orders of magnitude smaller than those of, for instance, the alkaline earth metals. To judge the accuracy of our approach we have therefore studied these differences as functions of pressure as shown in Fig. 8 from equilibrium down to a compression of 2.5. The results in Fig. 8 include the Madelung correction (11) which turns out to be crucial in the the comparison with recent pseudopotential and LMTO results (Moriarty 1982, Moriarty and McMahan 1982, McMahan and Moriarty 1983).

From Fig. 8 it is expected that the heavy alkalis at low temperature and pressure should form in the bcc structure while Li should be hcp. Experimentally it is known (Donohue 1975, Young 1975) that all five alkali metals at room temperature form in the bcc structure, and that they remain in this structure down to 5 [K] except Na which below 51 [K] transforms into the hcp structure and Li which at low temperature exhibits both an hcp and an fcc phase. Hence, except for Na the low pressure structures are correctly predicted.

Recently, Moriarty (1982) successfully estimated the structural stability for some 20 non-transition metals by means of his Generalized Pseudopotential Theory (GPT). He found incorrectly (see his Table VIII) that all the alkali metals at P = 0 and T = 0 should form in the hcp structure, but pointed out that at a slight compression the experimentally observed bcc structure would be stable in the heavy alkalies K, Rb, and Cs. A similar problem is encountered in another recent pseudopotential study (Young and Ross 1984) where the structures of Li and K at low temperature and pressure are predicted in agreement with experiment but where Na is expected to be fcc. On the other hand, in view of the extremely small energies involved, see Fig. 8, it is not surprising that the prediction of the low-pressure part of the alkali phase diagrams is a severe test of any calculation.

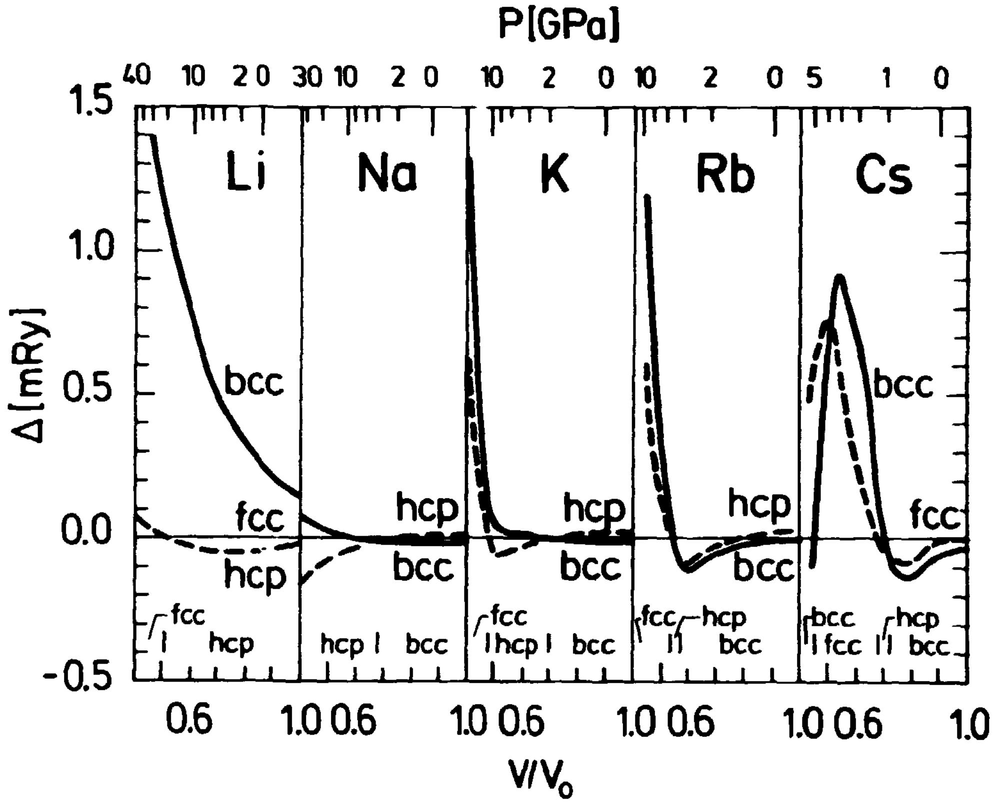

Fig. 8. Structural energy differences for the 5 alkali metals as functions of the relative volume V/V_0. At the top is given the calculated LMTO pressure P. The calculations included s,p, and d orbitals and the Madelung correction Eq. (11).

In their work on the third-row metals McMahan and Moriarty (1983) compared structural energy differences obtained by means of the LMTO and GPT methods and found excellent qualitative agreement except for Na. If we compare our Na results in Fig. 8 with their Fig. 1 we find somewhat surprisingly that our calculations are in closer agreement with their GPT than with their LMTO results. There are several reasons for the differences between the two LMTO calculations. Firstly, we have included the Madelung correction (11) without which the calculated bcc curve is entirely above and the hcp curve entirely below the fcc, in qualilitative agreement with their

LMTO results. Secondly, we have sampled the Brillouin zone on a finer mesh, i.e. 916, 819, and 448 points in the irreducible wedge for fcc, bcc, and hcp, respectively, and finally, we have improved the convergence of the reciprocal lattice sums in the expression for the combined correction terms (Andersen 1975) whereby the numerical errors in the structural energy differences for Na is below 0.01 mRy. As a result it appears that in the case of closely packed crystal structures the LMTO method including the Madelung correction (11) has an accuracy comparable to that attained by pseudopotential theory.

Owing to the inclusion of only three crystal structures in Fig. 8, Cs is incorrectly calculated to transform into the bcc structure at a compression of 2.2. However, in a recent study of Cs above the s-d transition, i.e. beyond the pressure range of the present work, McMahan (1984) found that Cs had transformed into the Cs IV structure before the bcc structure became more stable than fcc, in agreement with high pressure experiments (Takemura et al. 1981, 1982).

5.2. The alkali metals at moderate compression

According to Fig. 8 all the alkali metals should at low temperature be part of the same crystal structure sequence bcc→hcp→fcc, and one would anticipate that these transitions are driven by the pressure-induced lowering of initially unoccupied d states through the Fermi level, whereby electrons are gradually transferred from the s into the d band. If one plots the calculated crystal structures as functions of d occupation number as in Fig. 9 it is seen that only in the heavy alkalis K, Rb, and Cs is this mechanism at work while the transitions in Li and Na at least below 35 [GPa] have a different origin.

The experimental situation at room temperature has recently been summarized as follows (Takemura and Syassen 1983, Olijnyk and Holzapfel 1983). Li exhibits a bcc→fcc transition at 6.9 [GPa]

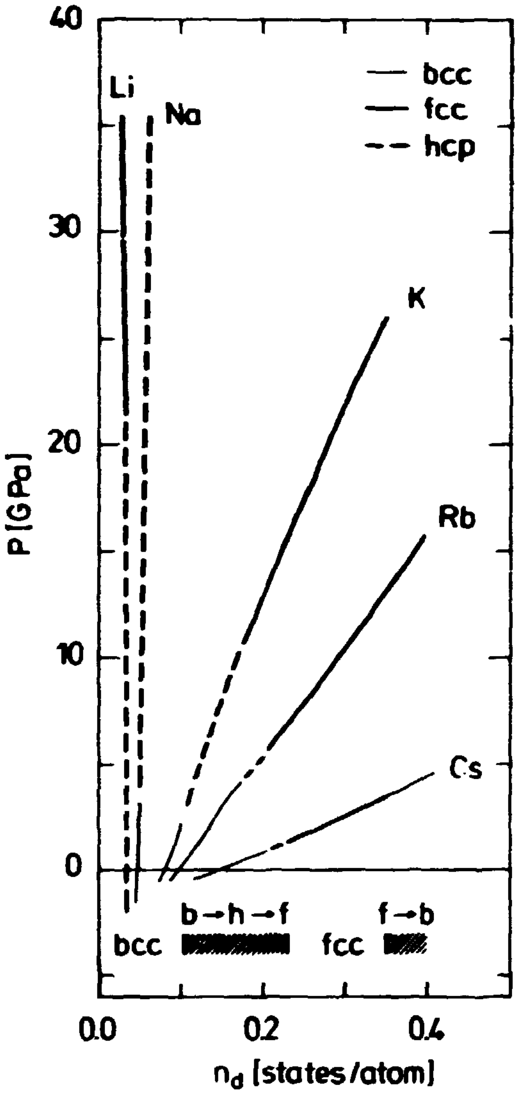

Fig. 9. Calculated crystal structures for the alkali metals as functions of the LMTO pressure and d occupation number.

(Olinger and Shaner 1983) while Na remains in the bcc structure up to at least 30 [GPa] (Alexandrov et al. 1982) which substantiates the notion that the s-d transition is unimportant in these two metals. The heavy alkalis all exhibit a bcc→fcc transition (K (Takemura and Syassen 1983, Olijnyk and

Holzapfel 1983), Rb (Takemura and Syassen 1982), Cs (Hall et al. 1964)) before they transform into more complex structures of which only the so-called Cs IV has been solved so far (Takemura et al. 1982).

To our knowledge there are no low-temperature high-pressure experiments which could substantiate the existence of the predicted bcc→hcp→fcc sequence, where according to Figs. 8 and 9 the hcp phase at least in K should be stable over an appreciable pressure range. However, in view of the fact that temperature at atmospheric pressure stabilizes the bcc phase to the extent that all the alkali metals are bcc above 100 K it is reasonable to assume that the intermediate hcp phase, which is only marginally stable, is also suppressed at higher temperatures. Thus, in a high-pressure experiment at room temperature one would see a direct bcc→fcc transition, as indeed one has observed (Hall et al. 1964, Takemura and Syassen 1982, 1983, Olijnyk and Holzapfel 1983). If the hcp phase is suppressed the best estimate of the room temperature bcc→fcc transition pressure is the critical pressure for the low-temperature hcp→fcc transition (cf. Fig. 8). We find the transition pressures to be 11, 5.5, and 1.4 [GPa] for K, Rb, and Cs, respectively, which should be compared to the experimental values of 11, 7, and 2.2 [GPa] listed in the references cited above.

Independent of whether the intermediate hcp phase exists or not, the high-pressure fcc phase in K, Rb, and Cs is much more stable than the initial bcc phase, see Fig. 8. Bardeen (1938) suggested already in 1938 that the transition observed at 2 [GPa] in Cs was from the normal bcc to an fcc phase and that it resulted from the nonelectrostatic interaction energy of the ions, the important term being the Born-Mayer (Born and Mayer 1932) repulsion between the ion cores. Here we shall show that the fcc phase in the heavy alkalies owes its stability directly to the pressure-induced s-d transition which is also shown to be behind, for instance, the isostructural fcc-fcc transition in Cs (Glötzel and McMahan 1979).

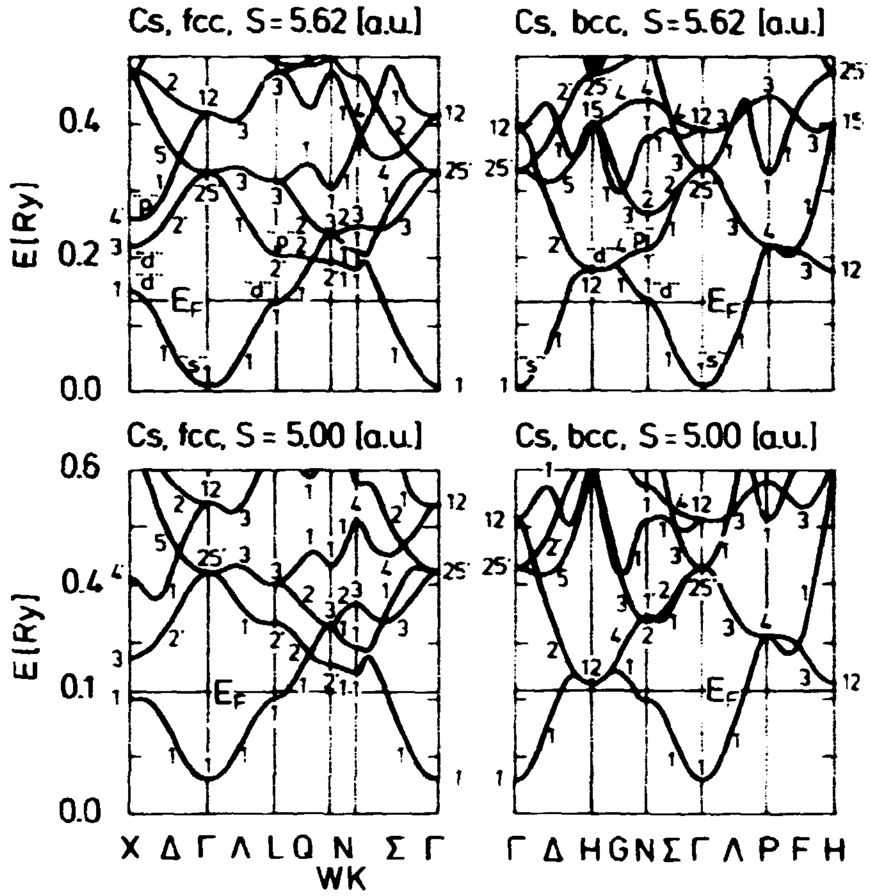

Cs, fcc, S = 5.62 [a.u.]

Cs, bcc, S = 5.62 [a.u.]

Cs, fcc, S = 5.00 [a.u.]

Cs, bcc, S = 5.00 [a.u.]

Fig. 10. Energy band structures for Cs at equilibrium, S = 5.62 [a.u.], and at a compressed volume, S = 5.0 [a.u.]. Conventional symmetry labels are given and the dominant s, p or d character is indicated at a few selected energy levels.

In Fig. 10 we compare the important parts of the fcc and bcc band-structures of Cs at the zero-pressure volume, V_0, and at the volume where the fcc phase becomes more stable than the initial bcc phase. The four band structures may be characterized as nearly free-electron and s-like below the Fermi level E_F and d-like above E_F. Typical d states have symmetry labels such as Γ_{12}, $\Gamma_{25'}$, H_{12}, and X_3, and they are seen to approach the Fermi level under compression. At $V = V_0$ the fcc and bcc band-structures are found to be extremely similar in the range below E_F which is important in the sums over occupied states in Eq. (9): They are both parabola shaped and "touch" E_F at a single symmetry point, L_1 for fcc and N_1 for bcc. As a result, the sum of the one-electron band-structure energies are almost equal and the main contribution to the stability of the bcc phase comes from the electrostatic Madelung term (11) which is negative, see Table 1.

At $V = 0.7\ V_0$ hybridization with the descending d band has moved the X_1 and neighbouring levels below E_F thereby lowering the energy in the fcc phase with respect to that in the bcc phase to the extent that the Madelung term is overcome and the structural energy difference is zero. Under further compression the X_1 level continues to descend and the fcc phase becomes increasingly stable, see Fig. 11. This trend is eventually broken because the maximum in the $\Gamma_1\Delta_1X_1$ band moves away from X and because the X_3 level drops below the Fermi level. Both effects de-stabilize the fcc structure and subsequently Cs transforms into the Cs IV phase. We shall not discuss this development here but refer to the experimental work of Takemura et al. (1982) and the theoretical treatment of McMahan (1984).

The presence of a gap at X (see Fig. 10) near the Fermi level in the compressed fcc phase which has no counterpart in bcc phase (nor in the hcp phase) stabilizes the fcc phase over the bcc in exactly the manner discussed by Jones in his classical work on the phase boundaries in binary alloys (Mott and Jones 1936, Jones 1937). The electron states below the gap have their one-electron band-energies lowered and are more densely populated than their free-electron or, here, bcc counterparts. The way the fcc phase is stabilized in Cs under pressure is shown in Fig. 11 where one notes that the stabilization occurs gradually from the point where the X_1 level crosses E_F. Hence, although the fcc phase eventually becomes more stable than the bcc phase because of the presence of the band gap at X, there is no direct relation between the volume ($V = 0.70\ V_0$) where the phase tran-

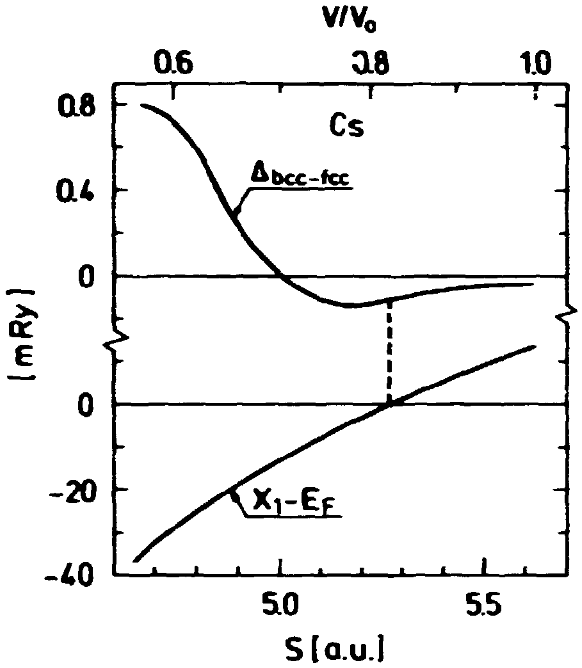

Fig. 11. Structural energy difference $\Delta_{bcc-fcc}$ for Cs, upper panel, and the position relative to the Fermi level, E_F, of the bottom of the gap at X in the fcc structure, lower panel, as functions of atomic radius, S, or relative volume V/V_0. $V = (4\pi/3)S^3$.

sition occurs and the volume ($V = 0.82\ V_0$) where the van Hove singularity connected with the X_1 level moves through the Fermi level. This delayed action is characteristic of many electronically driven transitions.

In the discussion of the stability of the fcc phase we have considered only Cs for simplicity, but examination of the bandstructures for K and Rb shows that the above picture applies equally well to these two metals although there are quantitative differences between K, Rb, and Cs caused by the fact that the zero-pressure position of the initially unoccupied d band drops relative to the Fermi level as the atomic number increases.

5.3. The alkaline earth metals

The calculated structural-energy differences for the alkaline earth metals under pressure are shown in Fig. 12. In the figure the metals are ordered according to their calculated d-occupation number at equilibrium and we have included the two divalent rare earths Eu and Yb, but excluded the divalent metals Be and Mg since they do not really belong to the crystal structure sequence we shall presently be discussing. The results at zero pressure for Be and Mg may, however, be found in the preliminary account (Skriver 1982) of the present work.

According to Fig. 12, Ca, Yb, and Sr at low temperature and pressure should form in the fcc structure while Eu, Ra, and Ba should be bcc. These predictions are in agreement with experiments (Donohue 1975, Young 1975) except for Yb which at low temperature takes up the hcp structure (Bucher et al. 1970). However, at a slightly expanded volume the hcp phase is calculated to be the stable phase, and hence one may not have to appeal to zero-point motion to explain the anomalous low-temperature hcp phase in Yb. Previous pseudopotential calculations (Animalu 1967) have explained the bcc structure in Ba and the pressure- (and temperature-) induced fcc→bcc transition in Sr, but gave an incorrect (bcc) zero-pressure crystal structure in Ca. Later pseudopotential results (Moriarty 1973) indicated that the stable structure at ordinary pressure should be the fcc structure for all the alkaline earths. Hence, it is still a challenge to pseudopotential theory to predict the crystal structures of the alkaline earth metals as a function of both atomic number and pressure.

There is a strong correlation between the calculated d occupation number and the calculated crystal structure as may be seen in Fig. 13. According to this the heavy alkaline earth metals should be part of the same hcp→fcc→bcc→hcp sequence. At zero pressure each individual metal may be characterized as being at different stages on the continuous s-to-d transition,

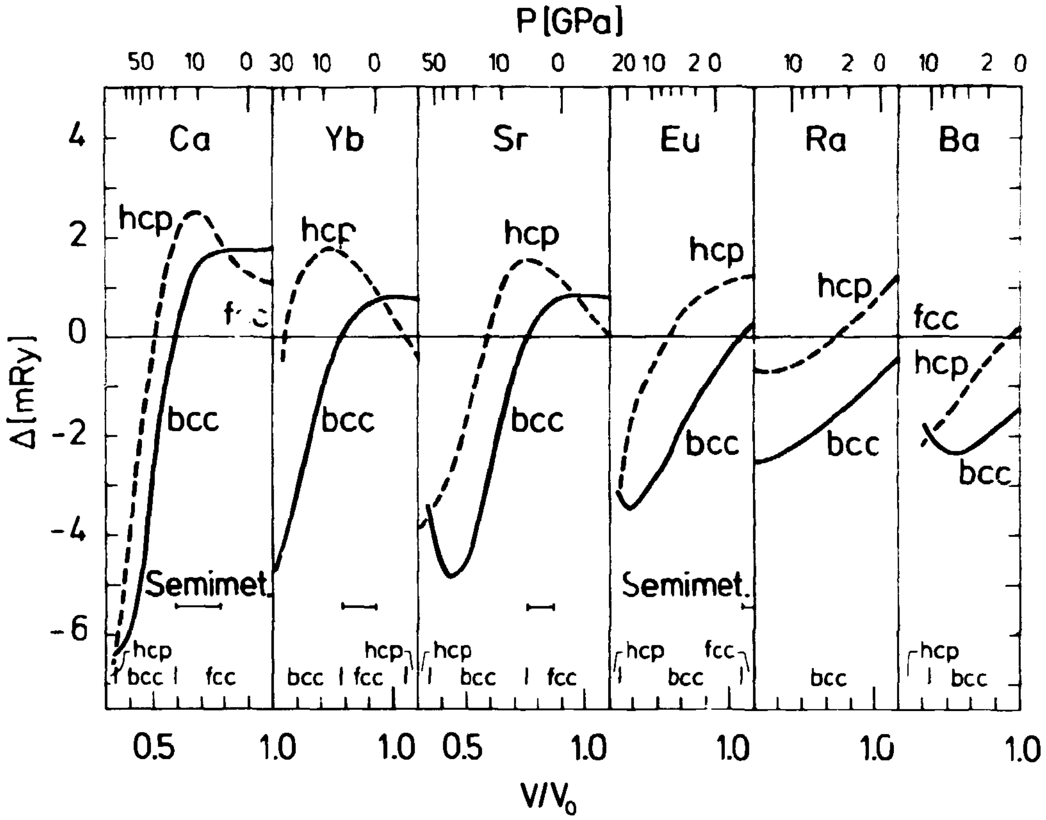

Fig. 12. Structural energy differences for the alkaline earth metals and the two divalent rare earths Eu and Yb as functions of relative volume V/V_0 and LMTO pressure P. The volume range over which the elements are calculated to be semimetallic is indicated by horizontal bars. The calculations included s, p, and d orbitals but not the Madelung correction Eq. (11).

i.e. by their d-occupation number, and the structural phase transitions are then driven by the pressure-induced lowering of the d band with respect to the s band. The correlation is, however, not perfect and the calculated crystal structure changes occur over a narrow range of d occupation numbers.

Experimentally (Jayaraman et al. 1963a,b, Jayaraman 1964, Olijnyk and Holzapfel 1984) one observes at room temperature the fcc→bcc part of the above sequence but the bcc→hcp transition

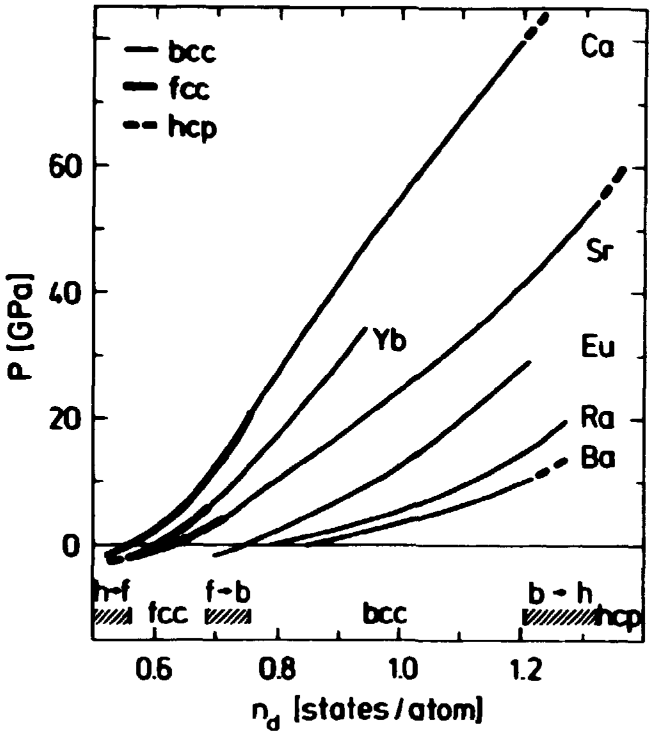

Fig. 13. Calculated crystal structures for the alkaline earth metals as functions of the LMTO pressure and d occupation number.

is found only in Ba whereas the lighter alkaline earth metals transform into more complex high-pressure phases (Olijnyk and Holzapfel 1984) not considered here. The critical pressures for the fcc→bcc transition in Ca, Sr, and Yb plus the bcc→hcp transition in Ba are calculated to be 21, 3.8, 5.5, and 10 [GPa], respectively (cf. Fig. 13). At room temperature Olijnyk and Holzapfel (1984) find experimentally 19.7 [GPa] for the transition in Ca while a low-temperature extrapolation of the high-pressure crystallographic measurements by Jayaraman et al. (1983a,b) and Jayaraman (1964) gives 4, 5, and 5 [GPa] for the latter three transitions. In view of the fact that no adjustable parameters have been used to construct Fig. 13, the agreement with the calculated critical pressures may be considered satisfactory.

The band-structure calculations show in agreement with the high-pressure resistivity data (Stager and Drickamer 1963a,b, Souers and Jura 1963, McWhan et al. 1963) that Ca, Sr, and Yb in the fcc phase should undergo a metal-semimetal-metal transition under pressure as described in detail for Ca by, for instance, Jan and Skriver (1981). Recently, Dunn and Bundy (1981) re-measured Ca and found the pressure range of the semimetallic phase to be much narrower than that found in earlier measurements (Stager and Drickamer 1963a) or predicted by band theory (McCaffrey et al. 1973, Mickish et al. 1974, Jan and Skriver 1981). Jan and Skriver (1981), for instance, predicted that fcc Ca should be semimetallic from 4 to 29 [GPa]. In the present extension of those calculations it is seen in Fig. 12 that before Ca reaches 29 [GPa] it is expected to transform into the bcc phase whereby the semimetallic behavious will be terminated already at 21 [GPa]. This termination of the semimetallic phase at approximately 20 [GPa] is in agreement with both resistivity (Dunn and Bundy 1981) and crystallographic (Olijnyk and Holzapfel 1984) measurements. However, the critical pressure of 4 [GPa] for the onset of the semimetallic behaviour is still too low compared to that obtained from the resistivity data of Dunn and Bundy (1981), and this discrepancy must be due to a failure of local-density theory of the kind mentioned by Jan and Skriver (1981).

In recent high-pressure measurements (Holzapfel et al. 1979, Takemura and Syassen 1985) both Eu and Yb are found to transform from the bcc to the hcp phase in seeming agreement with the systematics exhibited in Fig. 13. However, since Yb (Syassen et al. 1982) and presumably also Eu (Johansson and Rosengren 1975, Rosengren and Johansson 1976) change valence under pressure their high-pressure hcp phase is more appropriately thought of as belonging to the rare earth sequence, see Fig. 1, whereby it follows that Eu and Yb at very high pressures should exhibit the well-known hcp→Sm-type→dhcp→fcc transitions.

5.4. The transition metals

The calculated structural energy differences for the 3d, 4d, and 5d transition metals are shown in Fig. 14 and, as a comparison will show, the predicted crystal structures of all the metals included in this figure, neglecting the three ferromagnetic 3d metals, agree with the experimentally observed crystal structures, Fig. 1, except for the case of Au where the bcc structure is calculated to be marginally more stable than fcc. Hence, it follows that by including complete, i.e. fully hybridized, band-structures for each individual metal but still retaining the force theorem one has cured most of the problems connected with the simple canonical picture discussed in Sect. 1.2 and exemplified in Fig. 7. Furthermore, one should note that the correlation between crystal structure and d occupation which the canonical description predicts remains valid also for the complete calculations.

The results in Fig. 14 are very similar to those obtained by Pettifor (1970, 1972, 1977) for the 3d metals and by Williams and Janak (1982) for the 4d metals. However, in spite of the agreement of the theoretical calculations to within 25% and the correct prediction by the theory of the crystal structures of 27 metals, the calculated structural energy differences are found to be as much as a factor of 3-5 larger than the enthalpy differences obtained from the study of binary phase diagrams (Miedema and Niessen 1983), Fig. 15. At present the cause of this discrepancy is not known. The most likely candidates are either neglect of non-spherical terms in the charge density or a genuine failure of the local density approximation. The force theorem itself does not seem to be the cause of the discrepancy since Williams as quoted by Miedema and Niessen (1983) obtains results similar to ours by subtraction of total energy calculations. Finally, the "experimental" results derived by Miedema and Niessen (1983) are certainly model dependent and may therefore have large error bars.

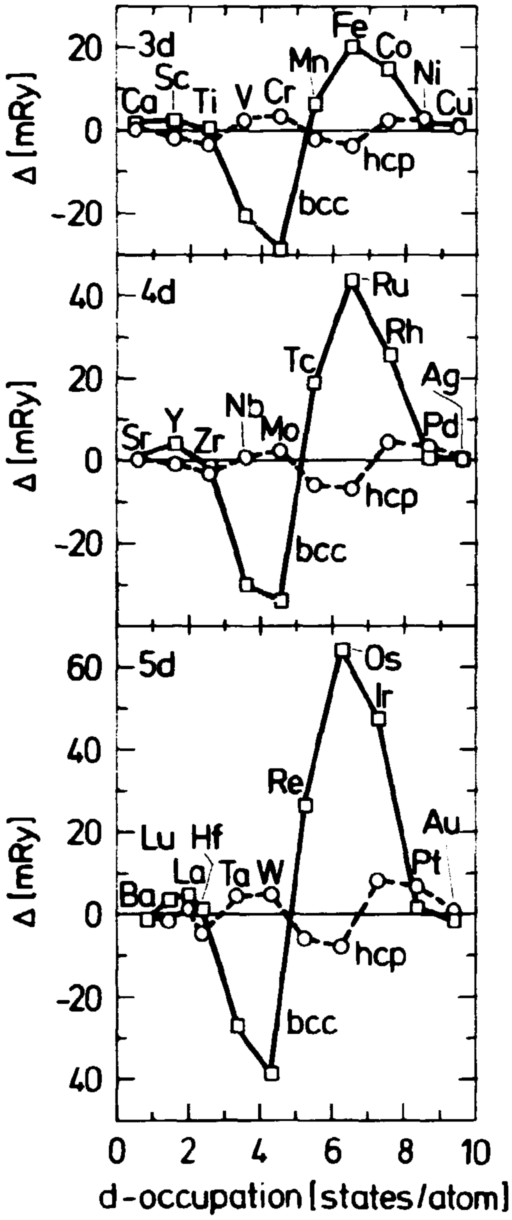

Fig. 14. Structural energy differences for the 3d, 4d, and 5d transition metals calculated at the experimentally observed equilibrium volume and plotted as functions of the d occupation numbers. The calculations included s, p, and d orbitals but not the Madelung correction Eq. (11).

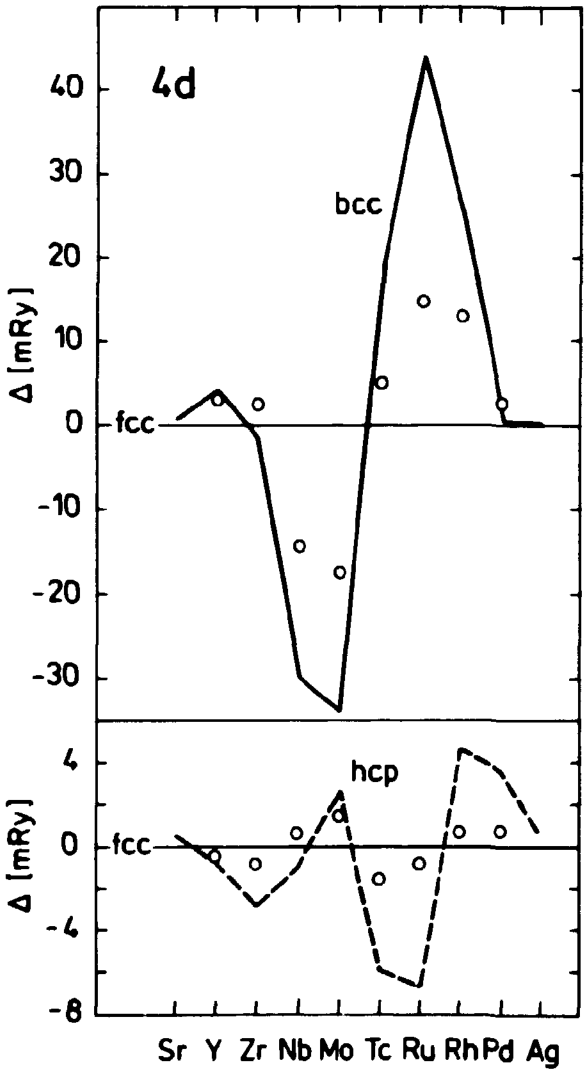

Fig. 15. The calculated bcc-fcc and hcp-fcc structural energy differences (solid and broken lines) for the 4d metals compared with the enthalpy differences derived from phase diagrams (Miedema and Niessen 1983), open circles.

5.5. The lanthanide metals

The calculated structural-energy differences for the two lanthanide metals La and Lu which bracket the lanthanide series are shown in Fig. 16. To compare directly with the canonical

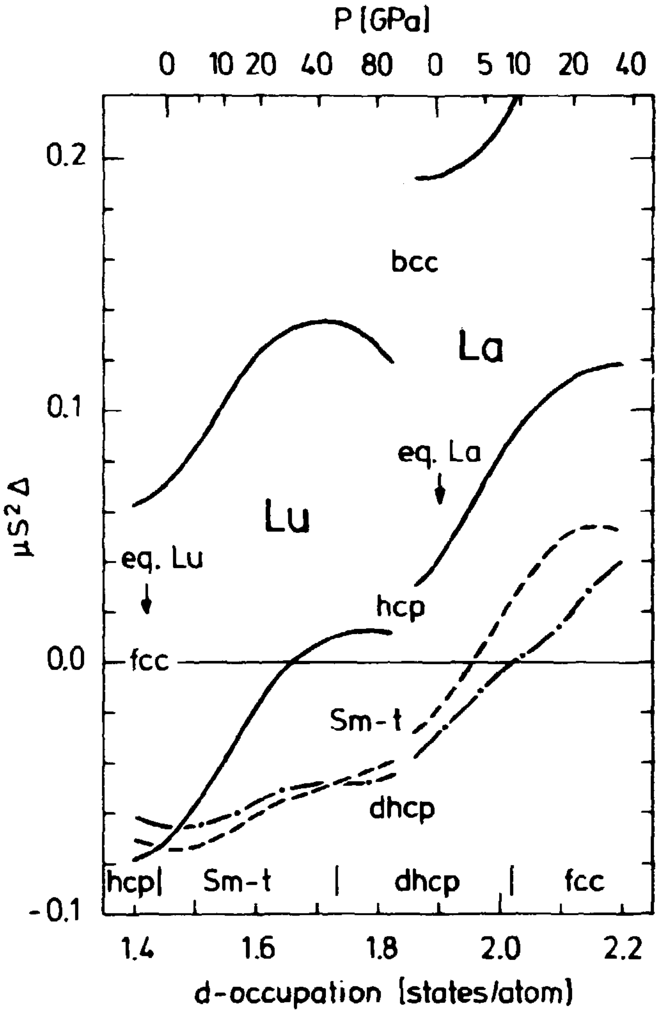

Fig. 16. Structural energy differences for La and Lu calculated as functions of pressure P and plotted versus d occupation number n_d. The calculations included s, p, d, and f orbitals, 4f for La and 5f for Lu, but not the Madelung correction Eq. (11).

results, Fig. 6, the energy differences have been brought onto the canonical scale and plotted as functions of the calculated d-occupation number. The results in Fig. 16 are qualitatively similar to the canonical results but the energy differences are generally smaller by approximately a factor of 2, judged by, for instance, the minimum in the Sm-type curve, than their canonical counterparts. Furthermore, the lanthanide sequence has been shifted to lower d-occupation numbers whereby the problems connected with the canonical description in the d occupation range above 1.6 have been removed. Hence, Ti, Zr, and Hf are no longer part of the lanthanide sequence and are instead correctly predicted to form in the hcp structure, Fig. 14.

In an account of the cohesive properties of the lanthanides Skriver (1983) found that the d-occupation numbers calculated at the experimentally observed equilibrium volume decreased approximately linearly with atomic number between La and Lu. Hence, Fig. 16 may be used to estimate the equilibrium crystal structures of the lanthanide metals, excluding Ce because of its γ-α transition, and the two divalent metals Eu and Yb. In agreement with the generalized phase diagram (Johansson and Rosengren 1975) we find that La, Pr, Nd, and Pm should form in the dhcp structure while Sm should be Sm-type. However, the heavy lanthanides are incorrectly estimated to form in the Sm-type structure. The immediate reason for this failure seems to be that the stability of the hcp structure at a given d occupation is calculated to be too low compared with dhcp and Sm-type but the deeper cause is not known at present. As a result, the Sm-type structure extends over too wide a d-occupation range.

Figure 16 may also be used to predict the behaviour of La and Lu under pressure. We find that Lu should transform from hcp to the Sm-type structure at - 2 [GPa] and into the dhcp structure at 35 [GPa]. Because of a 2% error in the calculated equilibrium radius and because of the failure mentioned above, the first estimate is in error by 25 [GPa], the experimental critical pressure being 23 [GPa] (Liu 1975). The second transition has not yet been observed.

Under pressure La is predicted to transform from dhcp to the fcc structure at 8 [GPa], Fig. 17, which compares favourably with the experimental room-temperature transition pressure of 2.5 [GPa] (Piermarini 1964). The distorted fcc phase discovered by

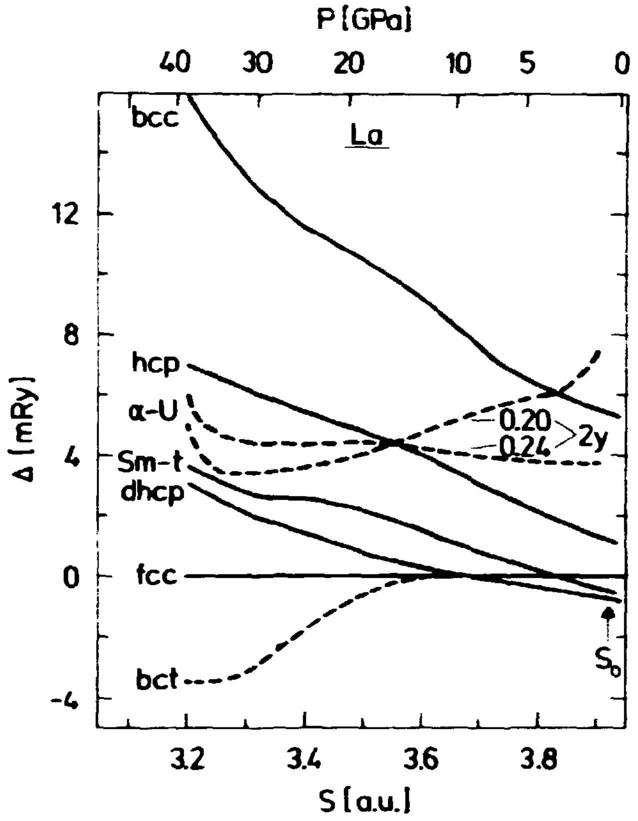

Fig. 17. Structural energy differences for La calculated as functions of pressure P and plotted versus atomic radius. The equilibrium radius S_0 = 3.92 [a.u.].

Grosshans et al. (1982) has not been considered, but we shall return to the high-pressure properties of La in the following section.

5.6. Cerium metal under pressure

The behaviour of Ce under pressure has been a subject of long-standing and some controversy, primarily because of the unusual isostructural γ→α transition. Here we shall be concerned with the fcc→α-U→tetragonal crystal-structure sequence exhibited by

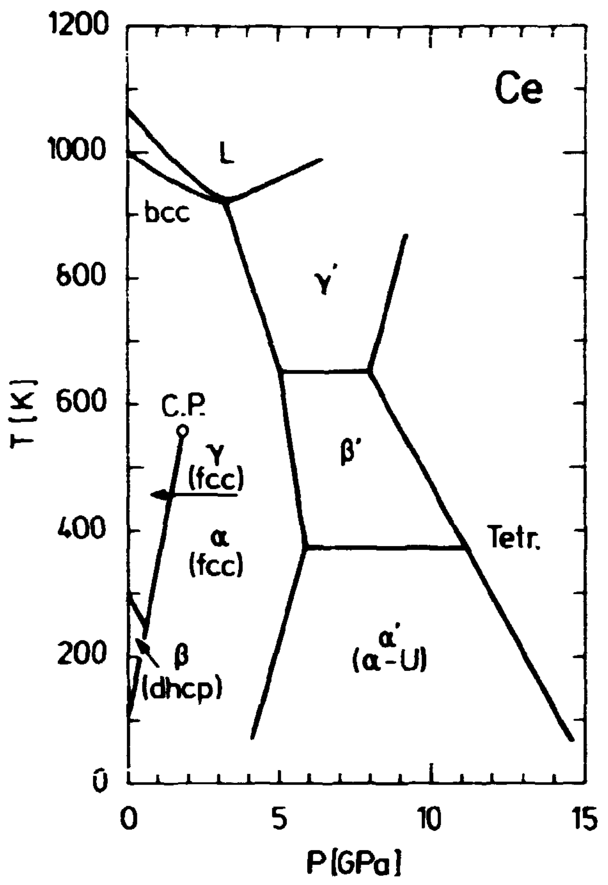

Fig. 18. Phase diagram for Ce compiled from Khvostantsev et al. (1983).

metallic Ce at low temperature in the pressure range up to 20 [GPa] (see Fig. 18). In the calculations we shall treat the s,p,d, and the 4f electrons on the same footing, i.e. as band electrons. Hence, we favour the picture of the $\gamma \rightarrow \alpha$ transition suggested by Gustafson et al. (1969) and elaborated by Johansson (1974) according to which pressure induces a Mott transition within the 4f shell such that the 4f electron goes from a localized state in γ-Ce to a delocalized, i.e. band state, in α-Ce.

According to the Mott-transition picture Ce metal at pressures above the $\gamma \rightarrow \alpha$ transition is different from the other lanthanides (and indeed from all the other metals we have considered so far)

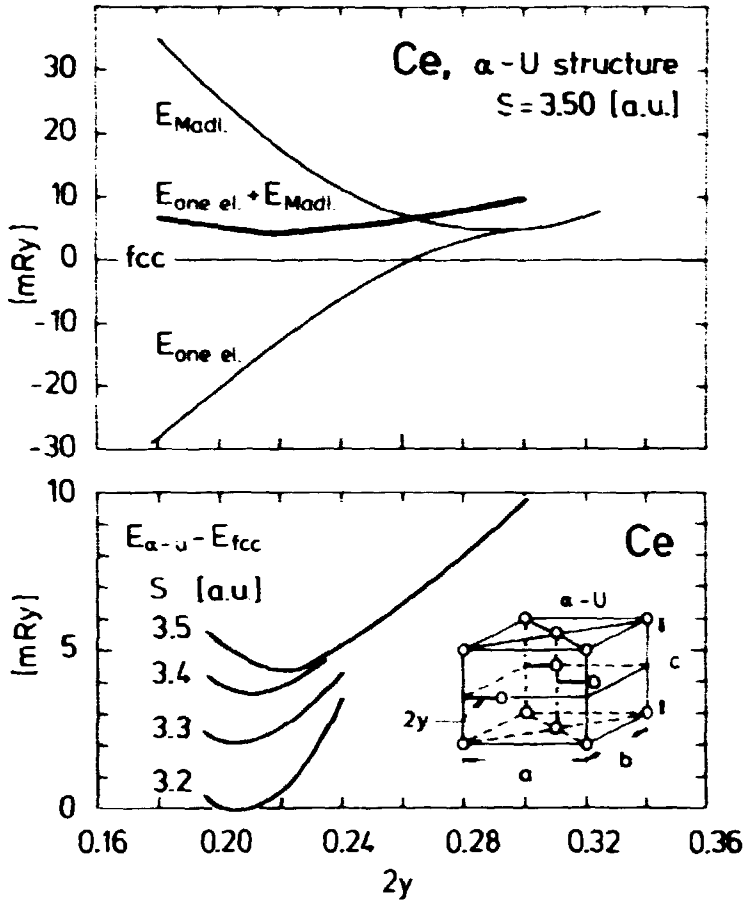

Fig. 19. Energy of Ce in the α-U structure relative to the fcc phase calculated as a function of the positional parameter 2y (see insert) and atomic radius S. The individual Madelung and one-electron contributions for one particular radius are shown in the upper panel.

in that it has a fourth conduction electron residing in the 4f band. It is this occupation of the 4f band which is expected to be responsible for the stability of the α-U structure found experimentally above 5.6 [GPa] (Ellinger and Zachariasen 1974) and perhaps for the tetragonal phase found above 12.1 [GPa] (Endo et al. 1977). To shed light on this question we shall now present a series of calculations of structural stabilities for Ce under pressure, and compare the results with those obtained for La where the 4f band is essentially empty.

The orthorombic α-U structure may be viewed as distorted fcc, where some of the face-centered atoms have been moved away from their positions as described by the parameter 2y, see Fig. 19. If 2y = 0.5a and a = b = c one has the usual fcc unit cell. In the case of Ce the Madelung contribution to the structural energy favours a 2y of approximately 0.3 (see top panel of Fig. 19) but the one-electron contribution moves the minimum in the energy difference to 2y = 0.21 which is the 2y value found experimentally in U (Donohue 1975). Under pressure the minimum is seen to move to slightly lower 2y values and eventually the α-U structure becomes more stable than the fcc.

From Fig. 19 it is expected that Ce will exhibit an fcc→α-U phase transition at a pressure which is calculated to be 11.7 [GPa]. The experimental transition pressure is 5.6 [GPa] (Ellinger and Zachariasen 1974), and the discrepancy may be attributed to the fact that the atomic sphere approximation is less suited for open crystal structures such as the α-U structure. As may be seen in Fig. 19 the Madelung correction, which we could neglect for the close-packed crystal structures of the alkaline earth and transition metals is now of the same order of magnitude as the one-electron contribution. Hence, inadequacies in the Madelung approximation of the electrostatic contribution to the structural energy are magnified and lead to errors in the estimate of the stability of the α-U structure. A similar problem was recently encountered in the case of the open Cs IV structure in Cs metal (McMahan 1984).

If we compare the structural energy-differences for Ce and La (Figs. 17,19) under pressure we find that while the α-U structure eventually becomes more stable than fcc in Ce it does not do so in La. Since the 4f band is essentially unoccupied in La, whereas Ce has approximately one 4f band electron, the notion that f-band states are responsible for the stability of distorted crystal structures such as the α-U structure is strongly supported by the present calculations. It follows that the α-U structure would not become stable in Ce under pressure unless

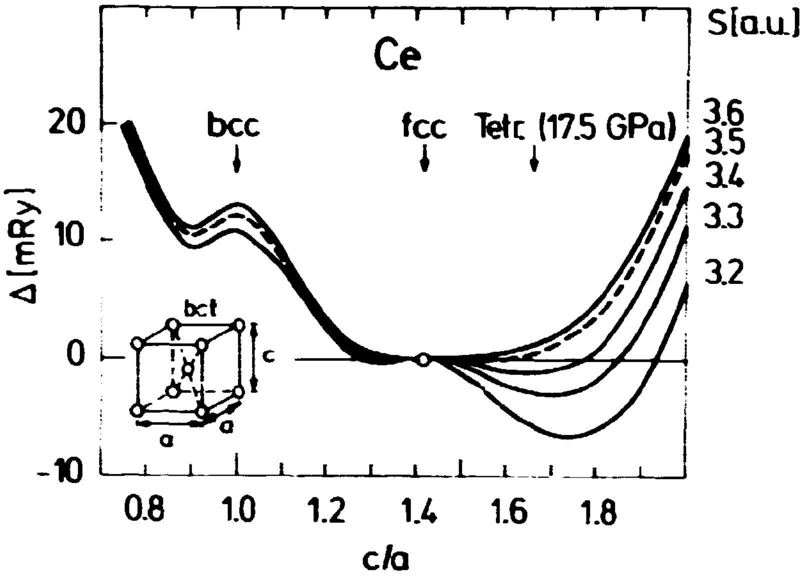

Fig. 20. Energy of Ce in the body-centred tetragonal (bct) structure relative to the fcc phase calculated as a function of the c/a ratio and atomic radius (the pressures can be inferred from Fig. 21). The insert shows the bct structure.

the 4f electrons were delocalized, i.e. band like, and therefore any adequate description of the α and α' phases in Ce must treat the 4f states on the same footing as the s,p, and d states. In short, Ce is a 4f band metal.

The high-pressure tetragonal structure (Endo et al. 1977) of Ce may be regarded as a distorted fcc structure in which the unit cell has been elongated along the c axis such that the c/a ratio in a body-centred tetragonal (bct) description is approximately 1.7, see Fig. 20. In the same description bcc and fcc correspond to c/a equal to 1 and √2, respectively. According to the structural energy differences in Fig. 20 Ce should as a function of pressure start out in the fcc structure and then transform into a bct structure with a c/a ratio which increases with pressure. In this case the 4f states do not seem to be responsible for the pressure-induced transition, since the same bct structure is also calculated to be the stable high-pressure phase of La, Fig. 17.

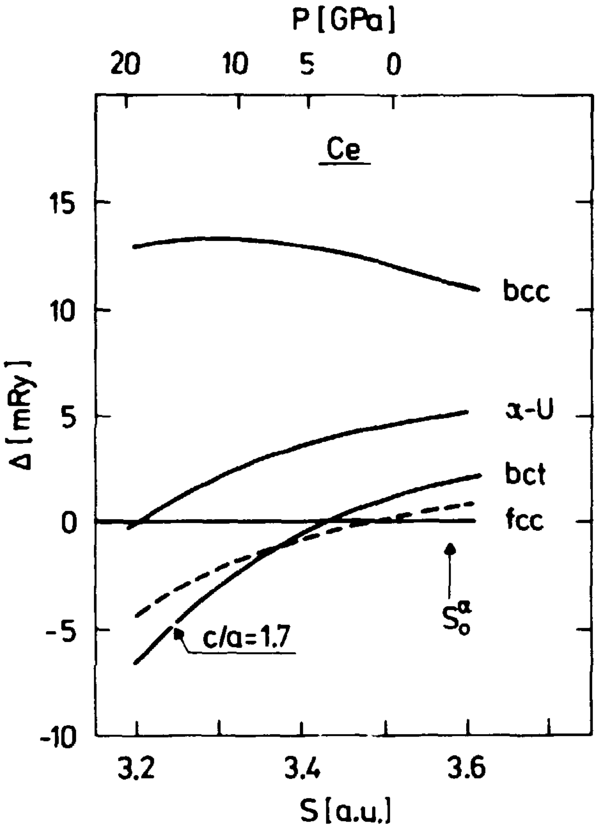

Fig. 21. Structural energy differences for Ce calculated as a function of pressure P and plotted versus atomic radius. S_0^α indicates the experimentally observed equilibrium radius of Ce in the α phase. The calculations included s, p, d, and f orbitals and the Madelung correction Eq. (11).

In Fig. 21 we have collected the calculated structural energy differences for Ce under pressure. Owing to the less accurate description of open structures discussed above, the α-U structure is seen not to be the stable phase in the pressure range considered, and instead Ce would be expected to go directly from the fcc into the bct phase. However, if we move the α-U curve down by 4.5 [mRy] which is 20% of the Madelung correction (see Fig. 19) we obtain agreement with experiment (Ellinger and Zachariasen 1974, Endo et al. 1977) in the sense that Ce is now expected to exhibit the crystal structure sequence fcc→α-U→tetragonal.

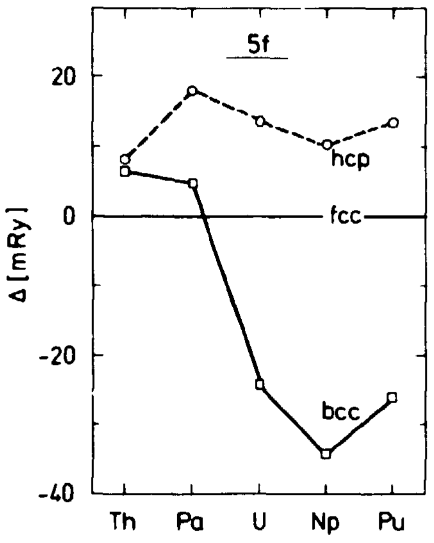

Fig. 22. Calculated structural energy differences for the light actinides plotted versus atomic number. The calculations included s, p, d, and f orbitals but not the Madelung correction Eq. (11).

5.7. The light actinides

The calculated structural energy differences for the light actinides Th-Pu are shown in Fig. 22, from which we deduce the most stable close-packed structure to be fcc in Th and Pa and bcc in U, Np, and Pu. This indicates that although these structures are not the stable low-temperature structures in Pa-Pu, they are at least close in energy to the distorted structures observed experimentally and may therefore be realized at elevated temperatures. Experimentally one finds the fcc structure to be stable in Th up to 1670 [K] (Donohue 1975, Young 1975), and there are indications that Pa has a high temperature fcc phase (Donohue 1975). Furthermore, neither U nor Np has a high temperature fcc phase but instead they become bcc before melting. Pu has a high temperature fcc (δ) phase but since this phase becomes unstable at a pressure of only 0.1 [GPa] it is most probably associated with a localization of the 5f electrons, and the relevant high temperature phase in the present context is then the bcc (ε) phase. Thus, experimentally the most stable close-packed structure appears to be fcc in Th and Pa, and bcc in U, Np, and Pu, in agreement with the findings in Fig. 22.

The low-temperature tetragonal structure (α) in Pa may be viewed (Zachariasen 1952) as a distorted bcc structure in which the unit cell has been compressed along the c axis such that the c/a ratio ratio is approximately 0.82, see Fig. 23. According to Fig. 23 the Madelung contribution favours bct structures with c/a in the range from 0.95 to 1.50, whereas structures with c/a outside this range rapidly become extremely unstable. In contrast, the one-electron contribution tends to favour c/a outside the central range, and as a result the energy difference curve for Th has one minimum at $c/a = \sqrt{2}$, corresponding to fcc, in agreement with experiment, while that of Pa exhibits three minima, one of which is close to the c/a observed experimentally in the α phase.

As in the case of the α-U structure in Ce, we are again experiencing problems stemming from the atomic sphere approximation and in particular the Madelung correction, which leads to slightly incorrect estimates of the structural energy differences for open crystal structures. Thus, in the case of Pa the most stable structure is calculated to be bct with c/a = 1.6, which incidentally is the high-pressure phase of Ce, whereas the minimum which corresponds to the experimental α structure lies 1.3 mRy above the absolute minimum and is shifted to a c/a of 0.92. However, in view of the rapidly changing Madelung correction in the range below c/a = 0.95, it is not unlikely that a better calculation of the electrostatic contribution to the structural energy differences may correct both errors.

Since the 5f band is unoccupied in Th while Pa has approximately one 5f electron it follows from Fig. 23 that the 5f states are responsible for the stability of the tetragonal α phase in Pa. Thus, the situation here is very similar to that

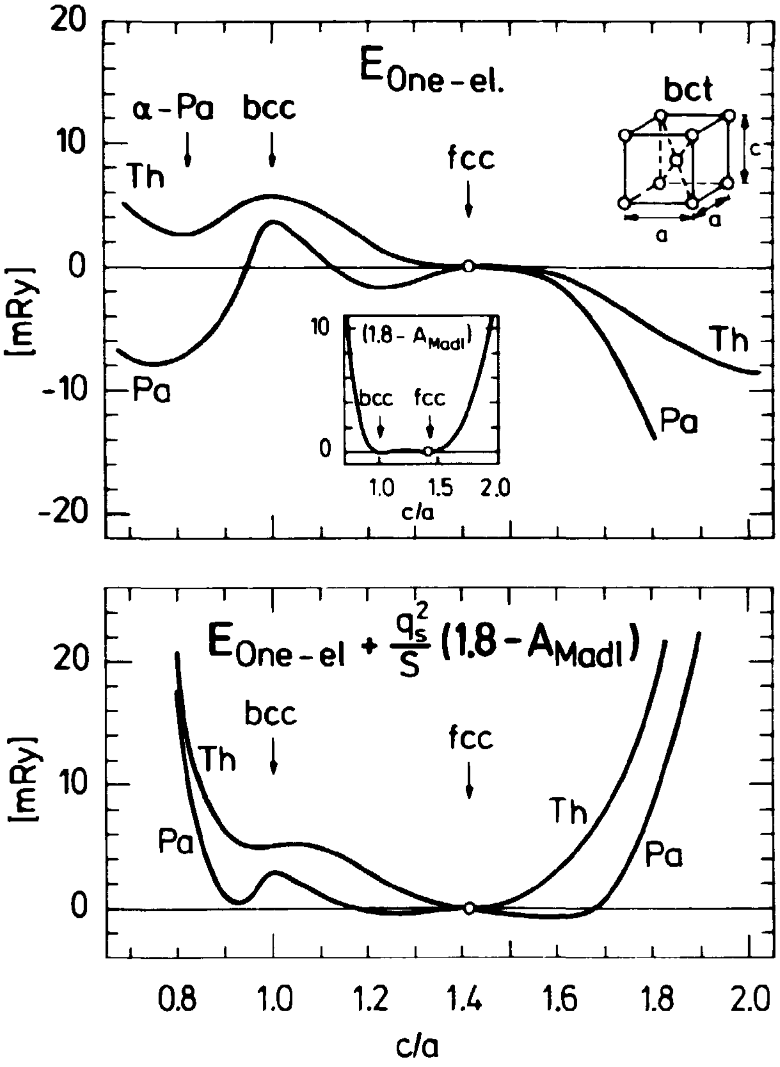

Fig. 23. Energy of Th and Pa in the bct structure relative to the fcc phase calculated as a function of the c/a ratio. The upper panel shows the one-electron contributions, the insert shows the shape of the Madelung correction, and the lower panel shows the total energy differences.

found earlier in Ce where the presence of one 4f electron stabilized the high pressure α-U structure, and again we take this to mean that the 5f states in the light actinides are itinerant, i.e. band-like, and give rise to distorted crystal structures.

6. CONCLUSION

We have studied the stability of the crystal structures of some 40 elemental metals within a one-electron approach. The effective one-electron equations have been solved self-consistently by means of the LMTO method and the structural energy differences calculated by means of Andersen's force theorem. This approach has the advantage of treating s, p, d, and f states on the same footing, thus leading to a conceptually consistent description of trends throughout the periodic table. However, the present implementation of the method is only accurate for close-packed crystal structures, and for that reason we exclude in our study open structures such as CsIV and the more exotic structures found in the actinide series. On the other hand, this shortcoming is not fundamental and will undoubtedly be remedied in the near future.

We find that the theory correctly predicts the crystal structures observed experimentally at low temperature and atmospheric pressure in 35 out of the 42 cases studied. In those few instances where the theory fails we find that the correct crystal structure is only marginally less stable than the calculated structure - this is the case for Na, Au, Yb, and Pa - or the metal is magnetic at low temperature, as in Mn, Fe, and Co. For the light actinides U, Np, and Pu we have not considered the experimentally most stable crystal structures but only the most stable close-packed structures and find the predictions of the theory to be in qualitative agreement with the known phase diagrams.

In a comparison between the calculated structural energy differences for the 4d transition metals and the enthalpy differences derived from studies of phase diagrams we find that, although the crystal structures are correctly predicted by the theory, the theoretical energy differences are up to a factor of 5 larger than their "experimental" counterparts. The reasons for this discrepancy may lie in the local-density approximation or in the neglect of the non-spherical part of the charge distribution. Furthermore, the derived enthalpy differences are certainly model dependent and may change as the model is improved.

In addition to the equilibrium properties we have studied the crystal structures of the alkali, the alkaline earth and some rare earth metals under pressure. We find that the heavy alkalis K, Rb, and Cs should be part of the crystal structure sequence bcc→hcp→fcc where the intermediate hcp phase may be suppressed at room temperature, and explain the experimentally observed bcc→fcc transition in terms of the pressure-induced descent of a zone-boundary energy gap which exists in the fcc band structure but has no counterpart in the bcc case. For the alkaline earth and rare earth metals we find crystal structure sequences which correlate with the calculated d-occupation numbers and which are in agreement with experimental high-pressure observations if we neglect some complex structures found in Ca and Sr.

Finally, we have studied the high-pressure crystal structure sequence fcc→α-U→tet. for La and Ce and find that under compression the α-U structure becomes more stable than fcc in Ce, but not in La. This indicates that the presence of itinerant 4f states is responsible for the fcc→α-U transition observed experimentally in Ce. In both La and Ce the calculations predict a tetragonal high-pressure phase. This phase is seen experimentally in Ce but not in La where one instead observes a distorted fcc structure not considered in the present work.

In conclusion, we have studied the stability of crystal structures of metals both at equilibrium and at high pressures by a one-electron approach. We find that we can account for the occurence of most of the close-packed structures observed experimentally. In the few cases where the theory is in disagreement with experiment we find that the correct crystal structure is only marginally less stable than the predicted structure. In order to describe open structures, such as α-U or CsIV, with the same accuracy as the close-packed structures one needs a more accurate approximation for the electrostatic contribution to the total energy.

7. ACKNOWLEDGMENT

The present series of calculations grew out of conversations with several people. It is thus a great pleasure to thank K. Syassen and K. Takemura for making me interested in the alkali metal problem, and B. Johansson for suggesting the Ce problem. B. Johansson and A.K. McMahan have furthermore helped clarify calculational as well as experimental problems. Part of this work was started while visiting Los Alamos Scientific Laboratory, and I wish to thank the group at the Materials Science Center for its kind hospitality. Finally, the present work has been supported by the Niels Bohr Foundation through the Royal Danish Academy of Sciences and Letters.

REFERENCES

AKELLA, J, Q. JOHNSON, W. THAYER, and R.N. SCHOCK (1979) J. Less-Comm. Met. 68, 95-97.

AKELLA, J, Q. JOHNSON, and R.N. SCHOCK (1980) J. Geophys. Res. B85, 7056-58.

ALEXANDROV, I.V., C.V. NESPER, V.N. KATCHINSKY and J. MARENKO (1982) paper presented at the 20th meeting of the European High Pressure Research Group, Stuttgart, 1982 (unpublished).

ANDERSEN, O.K. (1975) Phys. Rev. B12, 3060-83.

ANDERSEN, O.K. and O. JEPSEN (1977) Physica 91B, 317-328.

ANDERSEN, O.K., J. MADSEN, U.K. POULSEN, O. JEPSEN, and J. KOLLAR (1977) Physica 86-88B+C, 249-56.

ANDERSEN, O.K., H.L. SKRIVER, H. NOHL, and B. JOHANSSON (1980) Pure Appl. Chem. 52, 93-118.

ANIMALU, A.O.E. (1967) Phys. Rev. 161, 445-455.

BARDEEN, J. (1938) J. Chem. Phys. 6, 372-378.

BARTH, U. von and L. HEDIN (1972) J. Phys. C5, 1629-42.

BEAUDRY, B.J. and K.A. GSCHNEIDNER, JR. (1978) Preparation and Basic Properties of the Rare Earth Metals In: Handbook on the Physics and Chemistry of Rare Earths ed. by K.A. Gschneidner, Jr. and L.R. Eyring (North Holland, Amsterdam), 173-232.

BENEDICT, U., J.R. PETERSON, R.G. HAIRE, and C. DUFOUR (1984) J. Phys. F14, L43-L47.

BORN, M. and J.E. MAYER (1932) Z. Phys. 75, 1-18.

BREWER, L. (1967) Phase Stability in Metals and Alloys In: Phase Stability in Metals and Alloys ed. by P.S. Rudman, J. Stringer, and R.I. Jaffee. Batelle Institute Materials Science Colloquia, Switzerland, March 7-12, 1966,(McGraw-Hill, New York), pp. 39-62.

BUCHER, E., P.H. SCHMIDT, A. JAYARAMAN, K. ANDRES, J.P. MAITA, K. NASSAU, and P.D. DERNIER (1970) Phys. Rev. B2, 3911-17.

BROOKS, M.S.S and B. JOHANSSON (1983) J. Phys. F13, L197-L202.

DALTON, N.W. and R.A. DEEGAN (1969) J. Phys. C2, 2369-72.

DEEGAN, R.A. (1968) J. Phys. C1, 763-766.

DONOHUE, J. (1975) The Structures of the Elements (Wiley, New York), 436 p.

DUCASTELLE, F. and F. CYROT-LACKMANN (1971) J. Phys. Chem. Solids 32, 285-301.

DUNN, K.J. and F.P. BUNDY (1981) Phys. Rev. B24, 1643-50.

DUTHIE, J.C. and D.G. PETTIFOR (1977) Phys. Rev. Lett. 38, 564-567.

ELLINGER, F.H. and W.H. ZACHARIASEN (1974) Phys. Rev. Lett. 32, 773-774.

ENDO, S, H. SASAKI, and T. MITSUI (1977) J. Phys. Soc. Jpn 42, 882-885.

ESPOSITO, E., A.E. CARLSSON, D.D. LING, H. EHRENREICH, and C.D. GELATT, Jr. (1980) Phil. Mag. A41, 251-259.

FRIEDEL, J. (1969) Transition Metals. Electronic Structure of the d-band. Its Role in the Crystalline and Magnetic Structures In: The Physics of Metals 1. Electrons ed. by J.M. Ziman (Cambridge University Press, Cambridge), 340-408.

FRIEDEL, J. and C.M. SAYERS (1977) J. Phys. Orsay, Fr. 38, 697-705.

GLÖTZEL, D. and A.K. MCMAHAN (1979) Phys. Rev. B20, 3210-16.

GROSSHANS, W.A., Y.K. VOHRA, and W.B. HOLZAPFEL (1982) Phys. Rev. Lett. 49, 1572-75.

GSCHNEIDNER, K.A. (1964) Physical Properties and Interrelations of Metallic and Semimetallic Elements In: Solid State Physics vol. 16 ed. by H. Ehrenreich, F. Seitz, and D. Turnbull (Academic Press, New York), 275-426.

GSCHNEIDNER, K.A. and R.M. VALLETTA (1968) Acta Metall. 16, 477-484.

GUSTAFSON, D.R., J.D. MCNUTT, and L.O. ROELLIG (1969) Phys. Rev. 183, 435-440.

HAFNER, J. and V. HEINE (1983) J. Phys. F13, 2479-2501 and references therein.

HALL, H.T., L. MERRILL, and J.D. BARNETT (1964) Science 146, 1297-99.

HEINE, V. and D. WEAIRE (1970) Pseudopotential Theory of Cohesion and Structure In: Solid State Physics vol. 24 ed. by H. Ehrenreich, F. Seitz, and D. Turnbull (Academic Press, New York), 249-463.

HEINE, V. (1980) Electronic Structure from the Point of View of the Local Atomic Environment In: Solid State Physics vol. 35 ed. by H. Ehrenreich, F. Seitz, and D. Turnbull (Academic Press, New York), 1-127.

HODGES, C.H. (1967) Acta Metall. 15, 1787-94.

HOLZAPFEL, W.B., T.G. RAMESH, and K. SYASSEN (1979) J. Phys. Colloq. Orsay, Fr. 40, C5-390.

JAN, J.-P. and H.L. SKRIVER (1981) J. Phys. F11, 805-820.

JAYARAMAN, A., W. KLEMENT, Jr., and G.C. KENNEDY (1963a) Phys. Rev. Lett. 10, 387-389.

JAYARAMAN, A., W. KLEMENT, Jr., and G.C. KENNEDY (1963b) Phys. Rev. 132, 1620-24.

JAYARAMAN, A. (1964) Phys. Rev. 135, A1056-59.

JAYARAMAN, A. and R.C. SHERWOOD (1964) Phys. Rev., 134, A691-692.

JAYARAMAN, A. (1965) Phys. Rev. 139, A690-696.

JOHANSSON, B. (1974) Phil. Mag. 30, 469-482.

JOHANSSON, B. and A. ROSENGREN (1975) Phys. Rev. B11, 2836-57.

JOHANSSON, B. (1978) Structural and elastic properties of the f elements In: Rare Earths and Actinides, 1977 ed. by W.D. Corner and B.K. Tanner (IOP, Bristol), p. 39 (Inst. Phys. Conf. Ser. No. 37).

JONES, H. (1937) Proc. Phys. Soc. 49, 250-257.

KAUFMAN, L. and H. BERNSTEIN (1970) Computer Calculation of Phase Diagrams (Academic Press, New York), 334 p.

KHVOSTANTSEV, L.G. and N.A. NIKOLAEV (1983) Phys. Status Solidi (a)77, 161-166.

KOCH, C.C. (1970) J. Less-Common Met. 22, 149-173.

KOHN, W. and L.J. SHAM (1965) Phys. Rev. 140A, 1133-38.

LIU, L.-G., W.A. BASSETT, and M.S. LIU (1973) Science 180, 298-299.

LIU, L.G. (1975) J. Phys. Chem. Solids 36, 31-35.

MCCAFFREY, J.W., J.R. ANDERSON, and D.A. PAPACONSTANTOPOULOS (1973) Phys. Rev. B7, 674-684.

MACKINTOSH, A.R. and O.K. ANDERSEN (1980) The electronic structure of transition metals In: Electrons at the Fermi surface ed. by M. Springford (Cambridge University Press, Cambridge), 149-224.

MCMAHAN, A.K. and J.A. MORIARTY (1983) Phys. Rev. B27, 3235-51.

MCMAHAN, A.K. (1984) Phys. Rev. B29, 5982-85.

MCWHAN, D.B. and A.L. STEVENS (1965) Phys. Rev. 139, A682-689.

MCWHAN, D.B. and A.L. STEVENS (1967) Phys. Rev. 154, 438-445.

MCWHAN, D.B., T.M. RICE, and P.H. SCHMIDT (1969) Phys. Rev. 177, 1063-71.

MICKISH, D.J., A.B. KUNZ, and S.T. PANTELIDES (1974) Phys. Rev. B10, 1369-83.

MIEDEMA, A.R. and A.K. NIESSEN (1983) CALPHAD 7, 27-36.

MORIARTY, J.A. (1973) Phys. Rev. B8, 1338-45.

MORIARTY, J.A. (1982) Phys. Rev. B26, 1754-80.

MORIARTY, J.A. and A.K. MCMAHAN (1982) Phys. Rev. Lett. 48, 809-812.

MOTT, N.F. and H. JONES (1936) The Theory of the Properties of Metals and Alloys (Oxford University Press, London). 326 p.

NAKAUE, A. (1978) J. Less-Common Met. 60, 47-58.

NIEMINEN, R.M. and C.H. HODGES (1976) J. Phys. F6, 573-585.

OLIJNYK, H. and W.B. HOLZAPFEL (1983) Phys. Lett. 99A, 381-383.

OLIJNYK, H. and W.B. HOLZAPFEL (1984) Phys. Lett. 100A, 191-194.

OLINGER, B. and J.W. SHANER (1983) Science 219, 1071-72.

PETTIFOR, D.G. (1970) J. Phys. C3, 367-377.

PETTIFOR, D.G. (1972) Theory of the Crystal Structures of Transition Metals at Absolute Zero In: Metallurgical Chemistry. Proceedings of a symposium held July 14-16, 1971. Ed. by O. Kubaschewski (HMSO, London), 71.

PETTIFOR, D.G. (1976) Commun. Phys. 1, 141-146.

PETTIFOR, D.G. (1977) CALPHAD 1, 305-324.

PIERMARINI, G.J. and C.E. WEIR (1964) Science 144, 69-71.

ROOF, R.B., R.G. HAIRE, D. SCHIFERL, L.A. SCHWALBE, E.A. KMETKO, and J.L. SMITH (1980) Science 207, 1353-55.

ROOF, R.B. (1982) Z. Kristallogr. 158, 307-312.

ROSENGREN, A. and B. JOHANSSON (1976) Phys. Rev. B13, 1468-72.

SKRIVER, H.L. (1982) Phys. Rev. Lett. 49, 1768-72.

SKRIVER, H.L. (1983) Electronic Structure and Cohesion in The Rare Earth Metals In: Systematics and the Properties of the Lanthanides ed. S.P. Sinha (NATO ASI series on mathematical and physical sciences; C 109.) (Reidel, Company, Dordrect), 213-254.

SKRIVER, H.L. (1984) The LMTO Method (Springer, Berlin), 281 p.

SOUERS, P.C. and G. JURA (1963) Science 140, 481-483.

STAGER, R.A. and H.G. DRICKAMER (1963) Phys. Rev. 131, 2524-27.

STAGER, R.A. and H.G. DRICKAMER (1963) Science 139, 1284.

STEPHENS, D.R., H.D. STROMBERG, and E.M. LILLEY (1968) J. Phys. Chem. Solids 29, 815-821.

SYASSEN, K., G. WORTMANN, J. FELDHAUS, K.H. FRANK, and G. KAINDL (1982) Phys. Rev. B26, 4745-48.

TAKEMURA, K., S. MINOMURA, and O. SHIMOMURA (1981) Structure of Cesium and Iodine under Pressure In: Physics of Solids under High Pressure. Symposium held at Bad Honnef, FRG, August 10-14, 1981. Proceedings ed. by J.S. Schilling and R.N. Shelton (North-Holland, Amsterdam 1981), 131-135.

TAKEMURA, K. and K. SYASSEN (1982) Solid State Commun. 44, 1161-64.

TAKEMURA, K., S. MINOMURA, and O. SHIMOMURA (1982) Phys. Rev. Lett. 49, 1772-75.

TAKEMURA, K. and K. SYASSEN (1983) Phys. Rev. B28, 1193-96.

TAKEMURA, K. and K. SYASSEN (1985) J. Phys. F. in print.

WILLIAMS, A.R. and J.F. JANAK (1982) unpublished, and quoted by Miedema and Niessen (1983).

VOHRA, Y.K., H. OLIJNYK, W.A. GROSSHANS, and W.B. HOLZAPFEL (1981) Phys. Rev. Lett. 47, 1065-67.

YOUNG, D.A. (1975) Phase Diagrams of the Elements, Lawrence Livermore Laboratory Report UCRL-51902 (unpublished), 68 p.

YOUNG, D.A. and M. ROSS (1984) Phys. Rev. B29, 682-691.

ZACHARIASEN, W.H. (1952) Acta Cryst. 5, 19-21.

ZUNGER, A. and M.L. COHEN (1978) Phys. Rev. B18, 5449-72 and (1979) Ibid B20, 4082-4108.

Sales distributors:
G.E.C. Gad Strøget
Vimmelskaftet 32
DK-1161 Copenhagen K, Denmark

Available on exchange from:
Risø Library, Risø National Laboratory,
P.O.Box 49, DK-4000 Roskilde, Denmark

ISBN 87-550-1136-5
ISSN 0106-2840